

**Safety assessment of PPS.** After reference to the Japanese national guidelines for safety studies on medicinal products (rodent and nonrodent toxicity testing), continuous 2-month PPS infusions ranging from 110 to 460  $\mu\text{g}/\text{kg}/\text{day}$  were performed on each of four to seven adult mongrel dogs, Wistar rats, and Tg7 mice, using an Alzet osmotic pump and a brain infusion cannula. The blood cell count, coagulation, and serum chemistry were analyzed before PPS infusion was initiated and then each month thereafter. An electroencephalogram and 48-h spontaneous activity were recorded for the rats every 2 weeks from the time PPS infusion was started. Animals were sacrificed under deep anesthesia for histological evaluation of the brain when they reached an incurable condition or after the infusion had finished. Animal handling and sacrifice were in accordance with the national prescribed guidelines, and ethical approval for the studies was granted by the Animal Experiment Committee of Kyushu University.

**Statistical analysis.** Statistical significance was analyzed by repeated-measure analysis of variance followed by Scheffé's method for multiple comparisons.

## RESULTS

**Vehicle control.** Inoculation-related accidental death occurred within 1 week of postintracerebral inoculation and abnormal PrP deposition in the brain appeared at around day 35 postinoculation in Tg7 mice intracerebrally inoculated with 1% 263K homogenate. Accordingly, intraventricular infusion of a chemical was initiated either at an early stage (day 10) or at a late stage (day 35) of the infection in Tg7 mice. Continuous 4-week intraventricular infusion with vehicle alone from day 10 or 35 did not alter the mean incubation time (distilled water,  $51.6 \pm 1.8$  days [ $n = 5$ ] from day 10 and  $51.0 \pm 1.8$  days [ $n = 5$ ] from day 35; 25% dimethyl sulfoxide,  $52.3 \pm 2.1$  days [ $n = 5$ ] from day 10 and  $51.2 \pm 1.3$  days [ $n = 5$ ] from day 35; untreated,  $51.8 \pm 2.2$  days [ $n = 8$ ]).

**Antimalarial drugs, cysteine protease inhibitor, and amphotericin B.** Quinacrine (Fig. 1A), chloroquine (data not shown), and the E-64d cysteine protease inhibitor (data not shown) gave no prolongation effects. Overdose of quinacrine at more than 5  $\mu\text{mol}/\text{kg}/\text{day}$  from day 10, however, caused adverse effects and shortened the incubation period. Amphotericin B prolonged the incubation time at a dose of 9 or 90  $\mu\text{g}/\text{kg}/\text{day}$  from day 10 and gave about 26% prolongation of the mean incubation time (from 51 to 64 days) (Fig. 1B). With infusion from day 35, however, no significant prolongation was observed.

**PPS.** PPS showed the greatest beneficial effects among all of the chemicals examined in this study (Fig. 1C). Infusion at 460  $\mu\text{g}/\text{kg}/\text{day}$  from day 10 gave 141% prolongation (from 51 to 123 days), and even from the late stage (day 35), it gave 71% prolongation (from 51 days to 87 days).

The dose response of PPS was further examined at a later stage of the infection, day 42 (Fig. 2A). The dose response was in a bell-shaped distribution, and the maximal effect was observed at a dose of 230  $\mu\text{g}/\text{kg}/\text{day}$ , when the mean incubation time was prolonged by 29% (from 49 to 63 days).

The influence of infusion laterality on the outcome was examined by either ipsilateral or contralateral PPS administration to the inoculation site from day 10 or 35 postinoculation, but no significant difference according to the side of the infusion was observed (data not shown).

The relationship between the infusion initiation time and the outcome was analyzed (Fig. 2B). The effects of PPS were inversely correlated with time after inoculation. High-dose PPS infusion (460  $\mu\text{g}/\text{kg}/\text{day}$ ) at day 7 postinoculation prolonged the mean incubation period by 160% (from 47 to 122 days),

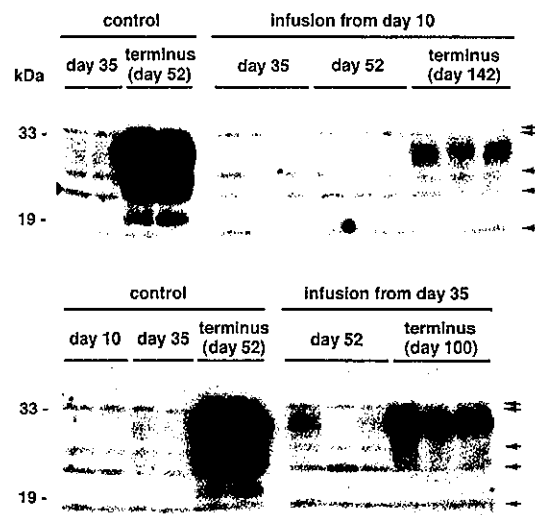


FIG. 4. PrPres in the brain with or without PPS treatment. Each lane represents an aliquot corresponding to 2.0 mg of brain tissue homogenate from an individual mouse sacrificed at a designated time. The brain tissue homogenate examined was prepared from the whole hemisphere contralateral to that of the inoculation site in either non-treated mice (control) or PPS-treated mice (infusion from day 10 or 35). In PPS-treated mice, the brain hemisphere examined was the side implanted with the intraventricular cannula. PPS was infused at 460  $\mu\text{g}/\text{kg}/\text{day}$  from day 10 or 35 postinoculation. Nonspecific signals that were observed without the primary antibody are shown by arrows.

while that at day 21 postinoculation prolonged it by 106% (from 47 to 97 days). Low-dose PPS infusion (110  $\mu\text{g}/\text{kg}/\text{day}$ ) showed a similar pattern but was less effective.

As a supplementary experiment to compare the efficacy of intraventricular administration with that of peripheral administration, 4-week continuous PPS infusion at 0.2, 2 or 20 mg/kg/day into a subcutaneous area of the back was performed with an osmotic pump from day 10 or 35 postinoculation. None of these treatments yielded any statistically significant effectiveness in prolonging the incubation time ( $51.0 \pm 1.8$  days [ $n = 4$ ],  $52.1 \pm 2.1$  days [ $n = 4$ ],  $52.3 \pm 1.6$  days [ $n = 5$ ], and  $23.8 \pm 16.5$  days [ $n = 5$ ] in the mice receiving 0, 0.2, 2, and 20 mg/kg/day from day 10, respectively;  $51.8 \pm 2.0$  days [ $n = 4$ ],  $51.0 \pm 1.8$  days [ $n = 4$ ],  $50.0 \pm 1.3$  days [ $n = 5$ ], and  $40.4 \pm 4.3$  days [ $n = 5$ ] in the mice receiving 0, 0.2, 2, and 20 mg/kg/day from day 35, respectively). However, treatment with the highest dose showed adverse effects, such as hemorrhage in the subcutaneous area surrounding the osmotic pump in 80% of the mice examined.

**PrP deposition and pathology.** Modification of abnormal PrP deposition and pathology in the brains of PPS-treated mice were analyzed (Fig. 3A and B). In the PPS-treated mice with an incubation period of 142 days, the brain hemisphere implanted with the PPS infusion cannula showed very faint or mild pathological changes, whereas the contralateral brain hemisphere was microscopically atrophied and accompanied by prominent spongiform degeneration and neuronal cell loss, especially in the cerebral cortex, hippocampus, and thalamus (Fig. 3A). Similarly, abnormal PrP deposition was prominently reduced within the brain hemisphere implanted with the infusion cannula, while abnormal PrP deposition was much en-

TABLE 1. Infectious titer and incubation time in the 263K-Tg7 model

Dilution	Mean incubation time <sup>a</sup> (days) ± SD	No. of diseased mice/total	Infectious titer <sup>b</sup> (log LD <sub>50</sub> /20 μl of tissue)	Corrected titer (log LD <sub>50</sub> /g of tissue)
10 <sup>1</sup>	43.8 ± 2.5	9/9	6.3	8.0
10 <sup>2</sup>	48.4 ± 3.1	10/10	5.3	7.0
10 <sup>3</sup>	55.6 ± 5.3	9/9	4.3	6.0
10 <sup>4</sup>	65.1 ± 2.9	8/8	3.3	5.0
10 <sup>5</sup>	76.0 ± 5.3	8/8	2.3	4.0
10 <sup>6</sup>	93.9 ± 17.0	10/10	1.3	3.0
10 <sup>7</sup>	158, 177, 422, 443	4/8	0.3	2.0
10 <sup>8</sup>	338, 555	2/7		
10 <sup>9</sup>		0/9		

<sup>a</sup> A 20-μl aliquot of serially diluted homogenate samples of the whole brain from a 263K-infected, terminally diseased Tg7 mouse was inoculated intracerebrally into Tg7 mice, and the mice were observed for up to 730 days postinoculation.

<sup>b</sup> The infectious titer was calculated by the Behrens-Kärber method.

hanced within the contralateral hemisphere, compared to the control mice with an incubation period of 52 days (Fig. 3B). GFAP immunoreactivity, indicating glial reaction, was similar to the PrP deposition.

In a sequential analysis of the control mice, cerebral PrP deposition had not appeared at day 10, first appeared in the cerebral white matter adjacent to the hippocampus at around day 35 in a coarse granular deposition pattern, and finally appeared in the thalamus, hypothalamus, and brain stem at terminus day 52 in a punctate pattern (Fig. 3C). Mice treated with PPS from day 10 did not show any PrP deposition within the hemisphere implanted with the cannula at day 52, and only punctate PrP deposition was observed in the brain stem at terminus day 142. Mice treated with PPS from day 35 demonstrated coarse granular PrP deposits in the cerebral white matter at day 52 within the cannula-implanted hemisphere, but there was no apparent PrP deposition in the thalamus at this stage. This PrP deposition pattern was similar to that in the control mice at day 35. Punctate PrP deposition was finally clearly visible in both the thalamus and the brain stem at terminus day 100.

**PrPres and infectivity.** PrPres was analyzed within the brain hemisphere implanted with the infusion cannula (Fig. 4).

PrPres signals in the control mice were very faint at day 35 but ultimately were very strong at terminus day 52. In mice treated with PPS from day 10, PrPres signals were not detected in the brain at day 35 or 52 but were detected at terminus day 142. However, the PrPres signals at day 142 did not reach the high level seen in the control mice at day 52. Similarly, in mice treated with PPS from day 35, the PrPres signals were very weak at day 52 and then increased at terminus day 100, but they still remained at a lower level than in the control mice.

Modification of the infectivity within the brain hemisphere implanted with the infusion cannula was clearly correlated with the level of PrPres (Tables 1 and 2). The infectious titer (log 50% lethal dose [LD<sub>50</sub>]/g of tissue) within the cannula-implanted brain hemisphere from terminally diseased mice was significantly decreased in the PPS-treated mice.

**PPS effects in other strains.** To investigate the effectiveness of PPS on pathogen strains other than 263K scrapie agent, Tga20 mice intracerebrally infected with 1% homogenates of RML scrapie agent or Fukuoka-1 Gerstmann-Sträussler-Scheinker disease agent were treated with a dose of 230 μg/kg/day for 4 weeks (Fig. 5). RML-infected mice treated with vehicle alone had a mean incubation period of 65 days, while those treated with PPS from day 14 or 49 postinoculation had a mean incubation period of 141 days (117% prolongation) or 95 days (46%), respectively. Similarly, Fukuoka-1-infected mice had a mean incubation period of 106 days, while those treated with PPS from day 14 or 49 postinoculation had a mean incubation period of 153 days (44% prolongation) or 133 days (25%), respectively. These data imply that intraventricular PPS infusion can be effective irrespective of the pathogen strain.

**Safety assessment of intraventricular PPS.** Thrombocytopenia and coagulation abnormality are known to occur occasionally with PPS, and PPS has been utilized in humans enterally, percutaneously, or intravenously but never intraventricularly. Thus, the safety of continuous intraventricular infusion should be evaluated before the possibility of application of this specific treatment to human patients is discussed. Continuous intraventricular infusion at doses ranging from 110 to 460 μg/kg/day was examined for 2 months in rodents (mice and rats) and nonrodents (dogs). Intraventricular infusion of up to

TABLE 2. Infectious titer in the brain with PPS treatment

Inoculum <sup>a</sup>	Mouse no.	Mean incubation time <sup>b</sup> (days) ± SD	Infectious titer <sup>c</sup> (log LD <sub>50</sub> /g of tissue)	Mean infectious titer ± SD <sup>d</sup>
Control	1	56.4 ± 0.5	8.9	8.87 ± 0.06*
	2	56.4 ± 1.6	8.9	
	3	57.2 ± 1.9	8.8	
PPS from: Day 35 postinoculation	1	62.4 ± 1.2	8.3	8.20 ± 0.10*
	2	63.4 ± 0.8	8.2	
	3	64.2 ± 5.6	8.1	
Day 10 postinoculation	1	69.8 ± 1.6	7.6	7.50 ± 0.14*
	2	71.4 ± 1.5	7.4	

<sup>a</sup> A 20-μl aliquot of a 0.1% homogenate from the infusion cannula-implanted brain hemisphere of each terminally diseased mouse was used for intracerebral inoculation into Tg7 mice.

<sup>b</sup> The data were collected from five inoculated mice in each group.

<sup>c</sup> The infectious titer was calculated from the incubation period based on the curve obtained from the data in Table 1 and corrected for the dilution power.

<sup>d</sup> \*, *P* < 0.01 versus the other groups.

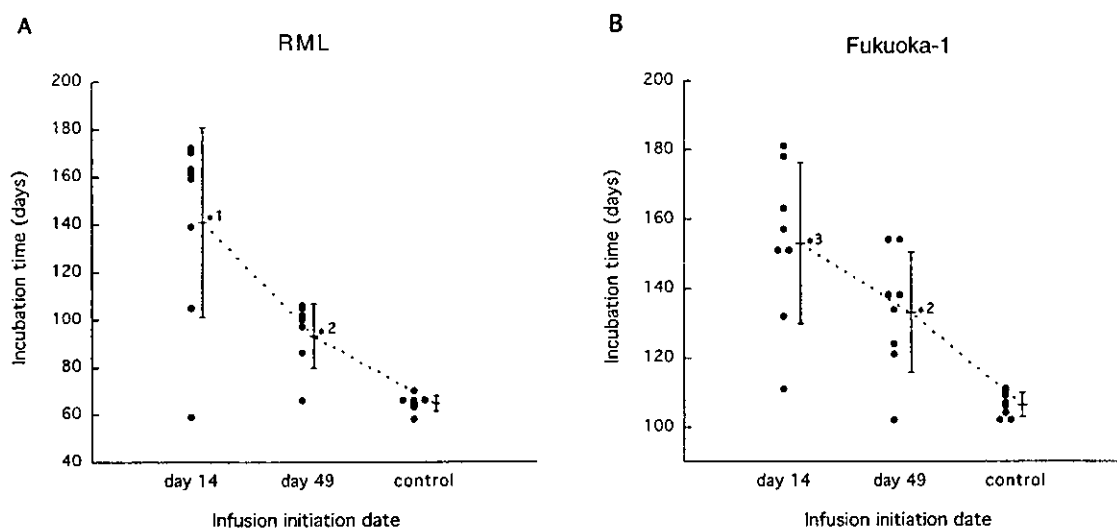


FIG. 5. Efficacy of PPS in mice infected with RML agent (A) or Fukuoka-1 agent (B). PPS at a dose of 230  $\mu\text{g}/\text{kg}/\text{day}$  was intraventricularly infused into intracerebrally infected Tga20 mice from day 14 or 49 postinoculation for 4 weeks. \*1,  $P < 0.01$  versus the other groups; \*2,  $P < 0.05$  versus the control; \*3,  $P < 0.01$  versus the control.

230  $\mu\text{g}/\text{kg}/\text{day}$  did not influence the data for the blood cell count, coagulation (Fig. 6), or serum chemistry, nor did it influence the electroencephalogram records, spontaneous activity pattern, behavior, or histological findings for the brain. However, higher doses showed adverse effects, but only in dogs. Three of the six dogs receiving 345  $\mu\text{g}/\text{kg}/\text{day}$  and all four dogs receiving 460  $\mu\text{g}/\text{kg}/\text{day}$  suffered partial or generalized seizures, which began within 24 h after PPS infusion was initiated. After treatment with anticonvulsants, the seizures of one dog from each group disappeared. The remaining five dogs did not recover from the seizures. Histologically, three of the five dogs had a large hematoma in the cerebral white matter where the cannula had been placed. None of the other dogs showed any notable pathological findings except for localized tissue damage and gliosis around the cannula route (data not shown).

## DISCUSSION

Here, we report on the effectiveness of clinically applicable chemicals by using a new drug evaluation system composed of gene-manipulated mice with substantially shorter disease incubation times and a continuous intraventricular infusion device. This system enabled us to evaluate the absolute therapeutic potency of chemicals in vivo within relatively short periods, regardless of their accessibility to the brain. Our observations indicate that two of the chemicals examined were effective in prolonging the incubation periods for intracerebrally infected animals. This suggests that intraventricular drug infusion could improve the prognosis of infected humans.

Among the chemicals examined here, PPS showed the most beneficial effects, and despite a limited infusion period, mice treated with PPS survived long after the infusion ended. Effectiveness was clearly observed even for the infusion at a late stage of infection, when abnormal PrP deposition was already visible in the affected brain. PPS is known to be effective in

inhibiting abnormal PrP formation in vitro (5) and/or in prolonging the disease incubation time in vivo (9, 12, 13, 16). However, its effectiveness in vivo has been restricted to administration either before or soon after peripheral infection. Thus, treatment with PPS has been thought of as being preventive only for those individuals with accidental inoculation in the periphery (7). Our observations, however, indicate that intraventricular PPS is in fact quite effective in prolonging the life spans of infected animals, even after abnormal PrP has already accumulated in the brain. The difference between previous observations and ours can be explained by poor or even no accessibility of peripherally administered PPS to the brain, and this is supported by our observation of the ineffectiveness of continuous subcutaneous PPS administration in intracerebrally infected mice.

The present studies revealed that PPS prevented not only new deposition of abnormal PrP but also the accumulation of neurodegeneration and infectivity. These findings suggest that prolongation of the life spans of infected animals by PPS could be due to its direct action on abnormal PrP generation. PPS interferes with the conversion of normal PrP molecules to abnormal ones by competitively binding to the PrP molecules (4, 5) and/or by altering the cellular localization of normal PrP molecules (20). PPS is also known to play a stimulatory role in the conversion of PrP molecules into protease-resistant ones in vitro (22). However, neither stimulatory effects on abnormal PrP accumulation nor acceleration of the disease course was observed in the present in vivo study.

From the histopathological studies, the effectiveness of PPS was clearly observed within the brain hemisphere where the intraventricular cannula was fitted, but not within the other hemisphere, in treated mice that survived long after the infusion had ended. This suggests that the infused PPS persisted around the infusion site and did not diffuse throughout the ventricular system, especially into the contralateral side of the brain. To obtain a much better outcome following PPS admin-

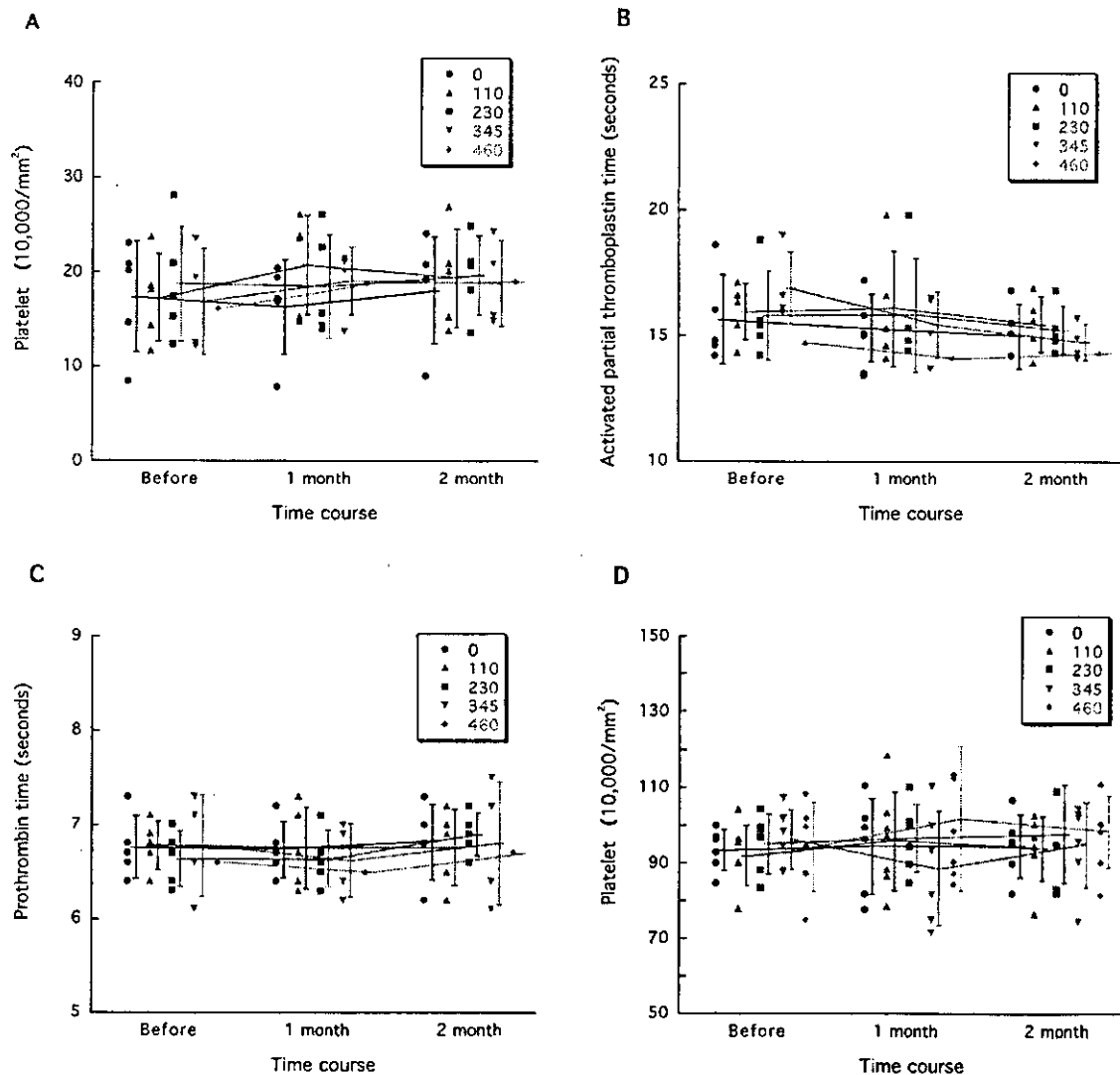


FIG. 6. Representative data from PPS safety assessment. Platelet counts in dogs and rats (A and D, respectively) and coagulation data for dogs (B and C) are shown. Each circle, triangle, square, inverted triangle, or diamond represents an individual animal. The data for two of the six dogs receiving 345  $\mu\text{g}/\text{kg}/\text{day}$  and for three of the four dogs receiving 460  $\mu\text{g}/\text{kg}/\text{day}$  were not obtained because they suffered seizures shortly after PPS infusion had been started and were sacrificed or died. However, the data for two dogs, one receiving 345  $\mu\text{g}/\text{kg}/\text{day}$  and the other receiving 460  $\mu\text{g}/\text{kg}/\text{day}$ , both of which suffered seizures but recovered, are included.

istration, it may be important to facilitate the diffuse distribution of PPS into every vulnerable area of the brain.

These studies also demonstrated that both the cerebral cortex and the hippocampus were apparently involved in the pathological conditions at the latest stage of the disease in the Tg7-263K model. Coarse granular PrP deposits in the cerebral white matter were the earliest abnormal finding in the affected brain, and these were followed by punctate PrP deposits in the brain stem, hypothalamus, and thalamus, but not in the cerebral cortex and hippocampus, in the nontreated mice. However, mice surviving long after intraventricular PPS infusion had devastating pathological changes in the cerebral cortex and hippocampus of the hemisphere opposite to that of the PPS infusion.

The PPS effects were quite dependent upon the timing of the infusion, and at a later disease stage or a terminal disease stage

the effects on prolongation of the life span were substantially limited. We have no precise knowledge as to when the mice used began to exhibit the very initial signs or symptoms of the disease, although we do know that abnormal PrP deposition in the brain began to be visible at around 5 weeks postinoculation and that the mice started to show definite signs about 2 days before death. Thus, our data do not guarantee similar effectiveness in human patients who already have signs and symptoms of the disease. On the other hand, the effectiveness of intraventricular PPS infusion was demonstrated not only for infection with the 263K strain but also for infection with two other distinct strains. These findings suggest that this treatment may have universal validity for TSE diseases.

PPS is utilized as a clinical medicine for interstitial cystitis, thrombophlebitis, and thrombosis, and its safety by enteral, percutaneous or intravenous administration has been clearly

established. Here, the safety of intraventricular PPS infusion at up to a dose yielding the maximal effectiveness in mice was demonstrated in experimental animals. However, at higher doses than this, there was a gap between small rodents and dogs, with the dogs showing adverse effects, such as seizures that were mostly caused by hematoma formation around the intraventricular cannula, although such adverse effects appeared only very early in the treatment. It is well known that smaller animals metabolize drugs much more quickly, and therefore intraventricular PPS at the same dosage was not toxic in mice and rats but was toxic in dogs. For application of this treatment to humans, it will be important to take account of the drug metabolism differences between mice and humans.

Amphotericin B and one of its derivatives are known to prolong the life spans of infected animals even with administration late in the disease course (8). In our experiments, however, amphotericin B did not cause any significant prolongation at a late-stage administration. Differences in the administration route, dose, and duration, as well as the experimental models, might account for this difference, but it remains to be elucidated.

Antimalarial chemicals, including quinacrine, had no effects in the present studies. These chemicals were previously found to be effective in inhibiting abnormal PrP formation in a scrapie-infected cell line (10, 15), and quinacrine has been used in clinical trials for TSE patients. However, together with the recent findings of two other research groups (1, 6), our data suggest that quinacrine may not improve the prognosis of the patients.

Finally, the placement of an intraventricular cannula in TSE patients may create public health issues due to fears of contamination of the operating room or safety issues with respect to the personnel involved with this procedure. For these reasons, other drug delivery systems which do not need a surgical procedure should be developed, and PPS derivatives that can be delivered into the brain after peripheral administration also need to be developed. As an immediately applicable remedy, however, continuous intraventricular PPS administration with an infusion device may be a candidate for a clinical trial, with a view to preventing the disease in those people categorized as being at extremely high risk or to improving the prognosis of diseased people with TSEs.

#### ACKNOWLEDGMENTS

This study was supported by grants to K.D. from the Ministry of Health, Labour and Welfare (H13-kokoro-025) and from the Ministry of Education, Culture, Sports, Science and Technology (13557118 and 14021085), Tokyo, Japan.

We thank B. Chesebro of the Rocky Mountain Laboratories, National Institute of Allergy and Infectious Diseases, National Institutes of Health, for providing the Tg7 mice and C. Weissmann of the Imperial College School of Medicine at St. Mary's, London, United

Kingdom, for providing the Tga20 mice. We also thank I. Goto for the electroencephalogram analyses.

#### REFERENCES

1. Barret, A., F. Tagliavini, G. Forloni, C. Bate, M. Salmons, L. Colombo, A. De Luigi, L. Limido, S. Suardi, G. Rossi, F. Auvré, K. T. Adjou, N. Salés, A. Williams, C. Lasmézas, and J. P. Deslys. 2003. Evaluation of quinacrine treatment for prion diseases. *J. Virol.* 77:8462–8469.
2. Brown, P. 2002. Drug therapy in human and experimental transmissible spongiform encephalopathy. *Neurology* 58:1720–1725.
3. Brown, P., M. Preece, J. P. Brandel, T. Sato, L. McShane, I. Zerr, A. Fletcher, R. G. Will, M. Pocchiari, N. R. Cashman, J. H. d'Aignaux, L. Cervenakova, J. Fradkin, L. B. Schonberger, and S. J. Collins. 2000. Iatrogenic Creutzfeldt-Jakob disease at the millennium. *Neurology* 55:1075–1081.
4. Caughey, B., K. Brown, G. J. Raymond, G. E. Katzenstein, and W. Thresher. 1994. Binding of the protease-sensitive form of PrP (prion protein) to sulfated glycosaminoglycan and Congo red. *J. Virol.* 68:2135–2141.
5. Caughey, B., and G. J. Raymond. 1993. Sulfated polyanion inhibition of scrapie-associated PrP accumulation in cultured cells. *J. Virol.* 67:643–650.
6. Collins, S. J., V. Lewis, M. Brazier, A. F. Hill, A. Fletcher, and C. L. Masters. 2002. Quinacrine does not prolong survival in a murine Creutzfeldt-Jakob disease model. *Ann. Neurol.* 52:503–506.
7. Dealler, S. 1998. Post-exposure prophylaxis after accidental prion inoculation. *Lancet* 351:600.
8. Demaimay, R., K. T. Adjou, V. Beringue, S. Demart, C. I. Lasmézas, J. P. Deslys, M. Seman, and D. Dormont. 1997. Late treatment with polyene antibiotics can prolong the survival time of scrapie-infected animals. *J. Virol.* 71:9685–9689.
9. Diringer, H., and B. Ehlers. 1991. Chemoprophylaxis of scrapie in mice. *J. Gen. Virol.* 72:457–460.
10. Doh-ura, K., T. Iwaki, and B. Caughey. 2000. Lysosomotropic agents and cysteine protease inhibitors inhibit scrapie-associated prion protein accumulation. *J. Virol.* 74:4894–4897.
11. Doh-ura, K., E. Mekada, K. Ogomori, and T. Iwaki. 2000. Enhanced CD9 expression in the mouse and human brains infected with transmissible spongiform encephalopathies. *J. Neuropathol. Exp. Neurol.* 59:774–785.
12. Ehlers, B., and H. Diringer. 1984. Dextran sulphate 500 delays and prevents mouse scrapie by impairment of agent replication in spleen. *J. Gen. Virol.* 65:1325–1330.
13. Farquhar, C., A. Dickinson, and M. Bruce. 1999. Prophylactic potential of pentosan polysulphate in transmissible spongiform encephalopathies. *Lancet* 353:117.
14. Fischer, M., T. Rulicke, A. Raeber, A. Sailer, M. Moser, B. Oesch, S. Brandner, A. Aguzzi, and C. Weissmann. 1996. Prion protein (PrP) with amino-proximal deletions restoring susceptibility of PrP knockout mice to scrapie. *EMBO J.* 15:1255–1264.
15. Korth, C., B. C. May, F. E. Cohen, and S. B. Prusiner. 2001. Acridine and phenothiazine derivatives as pharmacotherapeutics for prion disease. *Proc. Natl. Acad. Sci. USA* 98:9836–9841.
16. Ladogana, A., P. Casaccia, L. Ingrosso, M. Cibati, M. Salvatore, Y. G. Xi, C. Masullo, and M. Pocchiari. 1992. Sulphate polyanions prolong the incubation period of scrapie-infected hamsters. *J. Gen. Virol.* 73:661–665.
17. Priola, S. A., B. Caughey, and W. S. Caughey. 1999. Novel therapeutic uses for porphyrins and phthalocyanines in the transmissible spongiform encephalopathies. *Curr. Opin. Microbiol.* 2:563–566.
18. Prusiner, S. B. 1998. Prions. *Proc. Natl. Acad. Sci. USA* 95:13363–13383.
19. Race, R. E., S. A. Priola, R. A. Bessen, D. Ernst, J. Dockter, G. F. Rall, L. Mucke, B. Chesebro, and M. B. Oldstone. 1995. Neuron-specific expression of a hamster prion protein minigene in transgenic mice induces susceptibility to hamster scrapie agent. *Neuron* 15:1183–1191.
20. Shyng, S. L., S. Lehmann, K. L. Moulder, and D. A. Harris. 1995. Sulfated glycans stimulate endocytosis of the cellular isoform of the prion protein, PrP<sup>C</sup>, in cultured cells. *J. Biol. Chem.* 270:30221–30229.
21. Will, R. G., J. W. Ironside, M. Zeidler, S. N. Cousens, K. Estibeiro, A. Alperovitch, S. Poser, M. Pocchiari, A. Hofman, and P. G. Smith. 1996. A new variant of Creutzfeldt-Jakob disease in the UK. *Lancet* 347:921–925.
22. Wong, C., L. W. Xiong, M. Horiuchi, L. Raymond, K. Wehrly, B. Chesebro, and B. Caughey. 2001. Sulfated glycans and elevated temperature stimulate PrP(Sc)-dependent cell-free formation of protease-resistant prion protein. *EMBO J.* 20:377–386.

## Amyloid imaging probes are useful for detection of prion plaques and treatment of transmissible spongiform encephalopathies

Kensuke Ishikawa,<sup>1</sup> Katsumi Doh-ura,<sup>1†</sup> Yukitsuka Kudo,<sup>2</sup>  
Noriyuki Nishida,<sup>3</sup> Ikuko Murakami-Kubo,<sup>1</sup> Yukio Ando,<sup>4</sup>  
Tohru Sawada<sup>2</sup> and Toru Iwaki<sup>1</sup>

### Correspondence

Kensuke Ishikawa

kensuke@np.med.kyushu-u.ac.jp

Katsumi Doh-ura

doh-ura@mail.tains.tohoku.ac.jp

<sup>1</sup>Department of Neuropathology, Neurological Institute, Graduate School of Medical Sciences, Kyushu University, 3-1-1 Maidashi, Higashi-ku, Fukuoka 812-8582, Japan

<sup>2</sup>BF Research Institute Inc., Osaka 565-0873, Japan

<sup>3</sup>Department of Bacteriology, Nagasaki University School of Medicine, Nagasaki, 852-8501, Japan

<sup>4</sup>Department of Laboratory Medicine, Kumamoto University, Kumamoto 860-0081, Japan

Diagnostic imaging probes have been developed to monitor cerebral amyloid lesions in patients with neurodegenerative disorders. A thioflavin derivative, 2-[4'-(methylamino)phenyl] benzothiazole (BTA-1) and a Congo red derivative, (*trans, trans*),-1-bromo-2,5-bis-(3-hydroxycarbonyl-4-hydroxy)styrylbenzene (BSB) are representative chemicals of these probes. In this report, the two chemicals were studied in transmissible spongiform encephalopathies (TSE). Both BTA-1 and BSB selectively bound to compact plaques of prion protein (PrP), not only in the brain specimens of certain types of human TSE, but also in the brains of TSE-infected mice when the probes were injected intravenously. The chemicals bound to plaques in the brains were stable and could be detected for more than 42 h post-injection. In addition, the chemicals inhibited abnormal PrP formation in a cellular model of TSE with IC<sub>50</sub> values of 4 nM for BTA-1 and 1.4 µM for BSB. In an experimental mouse model, the intravenous injection of 1 mg BSB prolonged the incubation period by 14%. This efficacy was only observed against the RML strain and not the other strains examined. These observations suggest that these chemicals bind directly to PrP aggregates and inhibit new formation of abnormal PrP in a strain-dependent manner. Both BTA-1 and BSB can be expected to be lead chemicals not only for imaging probes but also for therapeutic drugs for TSEs caused by certain strains.

Received 24 October 2003

Accepted 2 March 2004

## INTRODUCTION

The transmissible spongiform encephalopathies (TSEs or prion diseases) form a group of fatal neurodegenerative diseases including bovine spongiform encephalopathy, Creutzfeldt–Jakob disease (CJD) and Gerstmann–Sträussler–Scheinker syndrome (GSS). These diseases are characterized by the accumulation in the brain of abnormal protease-resistant isoforms of prion protein (PrP), termed PrP<sup>Sc</sup> (Prusiner, 1991). The diseases are rare, but outbreaks of acquired forms of CJD, such as variant CJD (Will *et al.*, 1996) and iatrogenic CJD with cadaveric growth hormone or dura grafts (Hamad *et al.*, 2001), have prompted the development of therapeutic interventions and new diagnostic methods.

There are several drug candidates currently under clinical

trial for TSE patients, but unfortunately their potential usefulness remains limited. The problem is that these agents can only be given after the onset of the disease, often in the advanced stage, because there is no reliable means of detecting presymptomatic infection by either neuroimaging or laboratory examination. Some studies have reported that imaging assessments such as positron emission tomography (PET) with [<sup>18</sup>F]FDG and diffusion-weighted magnetic resonance imaging are useful for some types of human TSE (Demaerel *et al.*, 1997; Murata *et al.*, 2002), but are not always conclusive. At present, TSEs can be diagnosed with certainty only through pathological examination or immunoblotting of the diseased brain. Recently, PET and single photon emission CT (SPECT) using radiolabelled imaging probes, which provide information on neuropathological changes as well as brain metabolism, have been reported to be helpful for the early diagnosis of neurodegenerative disorders. A variety of chemicals have been evaluated for imaging β-amyloid (Aβ) aggregation, which is the major

<sup>†</sup>Present address: Department of Prion Research, Tohoku University Graduate School of Medicine, Sendai 980-8575, Japan.

hallmark of Alzheimer's disease. Candidate probes have primarily been derived from amyloid dyes such as thioflavin and Congo red (Bacskai *et al.*, 2002).

Here, we focused on two candidate probes: a thioflavin derivative, 2-[4'-(methylamino)phenyl] benzothiazole (BTA-1) and a Congo red derivative, (*trans, trans*),-1-bromo-2,5-bis-(3-hydroxycarbonyl-4-hydroxy)styrylbenzene (BSB) (Fig. 1). Both chemicals have been reported to detect amyloid or amyloid-like plaques in either post-mortem human brains or living mouse brains (Mathis *et al.*, 2002; Skovronsky *et al.*, 2000). Since PrP<sup>Sc</sup> tends to exist as amyloid-like fibrils, we used either BTA-1 or BSB to label PrP deposition in TSE brains. We also examined these chemicals for their application as therapeutics for TSE, since some amyloid-binding chemicals have the potential to inhibit PrP<sup>Sc</sup> propagation in *in vitro* and/or *in vivo* models of TSE (Supattapone *et al.*, 2002).

## METHODS

**Chemicals and experimental models.** BTA-1 was synthesized at Tanabe R & D (Saitama, Japan), and BSB was kindly provided by Dojindo Laboratories (Kumamoto, Japan). The chemicals were dissolved in 100% dimethylsulfoxide (DMSO) and stored at 4°C until use.

Three kinds of TSE-infected mouse neuroblastoma (N2a) cell lines were used in this study: N2a cells infected with the RML strain (ScN2a, Race *et al.*, 1988), N2a#58 cells infected with the 22L strain (L-1, Nishida *et al.*, 2000) and N2a#58 cells infected with the Fukuoka-1 strain (F-3). N2a#58 cells are known to express five times more normal PrP than N2a cells. All cell lines were individually cultured in Opti-MEM (Invitrogen; supplemented with 10% fetal calf serum).

For *in vivo* studies, transgenic mice models Tg7, over-expressing hamster PrP (Race *et al.*, 1995; Priola *et al.*, 2000), and Tga20, expressing five- to eightfold higher levels of murine PrP (Fischer *et al.*, 1996), were used. These models showed substantially shorter incubation periods following intracranial infection with 20 µl of 1% (w/v) 263K scrapie strain homogenate and RML strain, respectively. By 6 weeks post-inoculation, the Tg7 mouse model consistently showed plaque-type PrP deposition in the cerebral white matter between the cortex and hippocampus, and at the disease terminal stage showed synaptic-type deposition in the thalamus, hypothalamus and pons. Similarly, the Tga20 mouse model showed plaque-type deposition in the same brain areas, but not as consistently. Permission for the animal

study was obtained from the Animal Experiment Committee of Kyushu University. Each mouse weighed approximately 30 g, and was maintained under deep ether anaesthesia during all surgical procedures.

**PrP imaging in pathological sections.** Brain samples of autopsy-diagnosed sporadic CJD cases ( $n=3$ ), GSS cases ( $n=2$ ) and non-TSE control cases with amyloid lesions (Alzheimer's disease,  $n=2$ ) or without them (cerebral infarction,  $n=1$ ; pancreatic cancer,  $n=1$ ) were obtained from the Department of Neuropathology, Kyushu University. Tissue samples of TSE material were immersed in 98% formic acid for 1 h to reduce infectivity. Each tissue sample was embedded in paraffin, and then cut into 7 µm thick sections. Sections of variant CJD brain were kindly provided by James W. Ironside of the CJD Surveillance Unit, Edinburgh, UK. For neuropathological staining, sections were deparaffinized in xylene and hydrated in ethanol. They were then incubated for 30 min in a solution of 1 µM BTA-1 in 50% ethanol, rinsed and examined under a fluorescent microscope (DMRXA, Leica Instruments) with a UV filter set. The sections were washed overnight in 50% ethanol. After verifying clearance of the BTA-1 signal, they were incubated for 30 min in a solution of 1 µM BSB and re-examined under the fluorescent microscope. For comparison, each section was subsequently immunostained as described previously (Doh-ura *et al.*, 2000). Briefly, sections were incubated in 0.3% H<sub>2</sub>O<sub>2</sub> in absolute methanol for 30 min and then treated by a hydrolytic autoclave procedure (1 mM HCl, 121°C, 10 min). After rinsing with 50 mM Tris/HCl, pH 7.6, the sections were incubated at 4°C overnight with a rabbit primary antibody c-PrP, which was raised against a mouse PrP fragment, amino acids 214–228 (1:200; Immuno-Biological Laboratories, Gunma, Japan) (Yokoyama *et al.*, 2001), followed by incubation with a horseradish-peroxidase-conjugated secondary antibody (1:200; Vector Laboratories) at room temperature for 1 h. The coloured reaction product was developed with 3,3'-diaminobenzidine tetrahydrochloride solution. In addition, formalin-fixed brains of diseased Tg7 mice were investigated using the same procedure. To ensure specificity of the anti-PrP antibody, brain sections with other amyloid lesions such as senile plaques were also immunostained. No positive reactions were obtained.

**PrP imaging in presymptomatic mice.** BTA-1 or BSB 10–30 mg (kg body weight)<sup>-1</sup> in 10% DMSO/saline, or vehicle alone, was administered intravenously into Tg7 mice intracerebrally infected with the 263K strain at 6 weeks post-infection, or into Tga20 mice intracerebrally infected with the RML strain at 8 weeks post-infection. At this point the mice showed no apparent clinical signs of disease. As another control, either chemical was similarly injected into uninfected transgenic mice. The animals were sacrificed at different time-points, and the brains were removed, frozen in powdered dry ice and cut coronally into 10 µm thick sections using a cryostat. The sections were examined under a fluorescent microscope, and then analysed immunohistochemically for PrP as described above.

**PrP<sup>Sc</sup> inhibition in scrapie-infected cells.** PrP<sup>Sc</sup> inhibition assays using a cellular model of TSE were performed as described previously (Caughey & Raymond, 1993). Either BTA-1 or BSB in 100% DMSO was added at the designated concentrations to each of the cell lines in 6-well plates when they reached 5% confluency. The final concentration of DMSO in the medium was kept to less than 0.2%. Two controls, one for untreated cells and the other for cells treated with vehicle alone (0.2% DMSO), were prepared. The cultures were allowed to grow to confluence, and then harvested and analysed for PrP<sup>Sc</sup> content by immunoblotting. Briefly, the cells were lysed with lysis buffer (0.5% sodium deoxycholate, 0.5% Nonidet P-40, PBS) and digested with 20 µg proteinase K ml<sup>-1</sup> for 30 min at 37°C. The digestion was terminated with 0.5 mM phenylmethylsulfonyl fluoride, and the samples were centrifuged at 100 000 g for 30 min at 4°C. Pellets were resuspended in 30 µl of sample loading buffer and boiled for 5 min. The samples were separated on a 15%

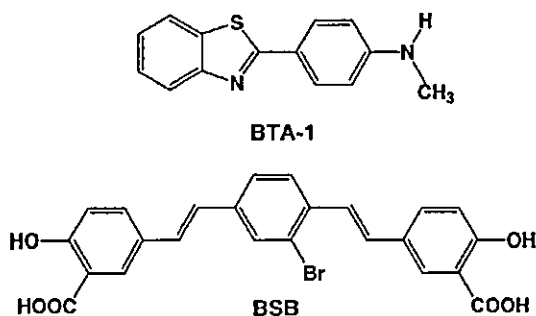


Fig. 1. Structures of the chemicals used in this study.

polyacrylamide Tris/glycine SDS gel and transferred to a PVDF filter (Millipore). PrP<sup>Sc</sup> was detected using a rabbit polyclonal antibody PrP-2B, which was raised against a mouse/hamster PrP fragment, amino acids 89–103 (1:5000) (Murakami-Kubo *et al.*, 2004), followed by an alkaline phosphatase-conjugated goat anti-rabbit antibody (1:20 000; Promega). Immunoreactive signals were visualized using the CDP-Star detection reagent (Amersham) and analysed densitometrically using image analysis software. More than two independent assays were performed for each experiment.

**Therapeutic treatment in model animals.** BSB dissolved in 10% DMSO/saline at 1 mg per injection was given intravenously to infected Tg7 mice ( $n=5$  in each group) or infected Tga20 mice ( $n=7$  in each group). The treatment was performed for Tg7 mice at 35 days post-infection (p.i.) and 50 days p.i., and for Tga20 mice at 45 days p.i. and 60 days p.i. Two control groups were prepared for both experimental models: untreated mice and mice treated with vehicle alone. The animals were monitored 5 days a week until the obvious clinical stage was reached, which was the day before or the day of death in Tg7 mice and 4–5 days before death in Tga20 mice. The statistical significance was analysed by one-way ANOVA followed by Scheffé's method for multiple comparisons.

## RESULTS

### Imaging of PrP deposition *in vitro* and *in vivo*

Imaging of PrP deposition in the brain by BTA-1 or BSB was first examined using histopathological specimens from human TSE cases. Both chemicals fluorescently labelled most of the compact PrP plaques in the cerebellar cortices of GSS cases (Fig. 2a and c). No residual fluorescence of BTA-1 was seen after thorough washing (Fig. 2b). The labelling intensity was stronger in the sections labelled with BSB compared with those labelled with BTA-1, but the size of each plaque detected by BTA-1 was on average larger than that detected by BSB. The plaques were counterstained with an antibody against the C terminus of PrP (Fig. 2d). In the sections from a variant CJD case, dense PrP plaques were detectable by both chemicals, whereas most of the immunopositive PrP deposits, such as fine granular deposits and perivacuolar deposits, were not labelled (Fig. 2e–h). In the

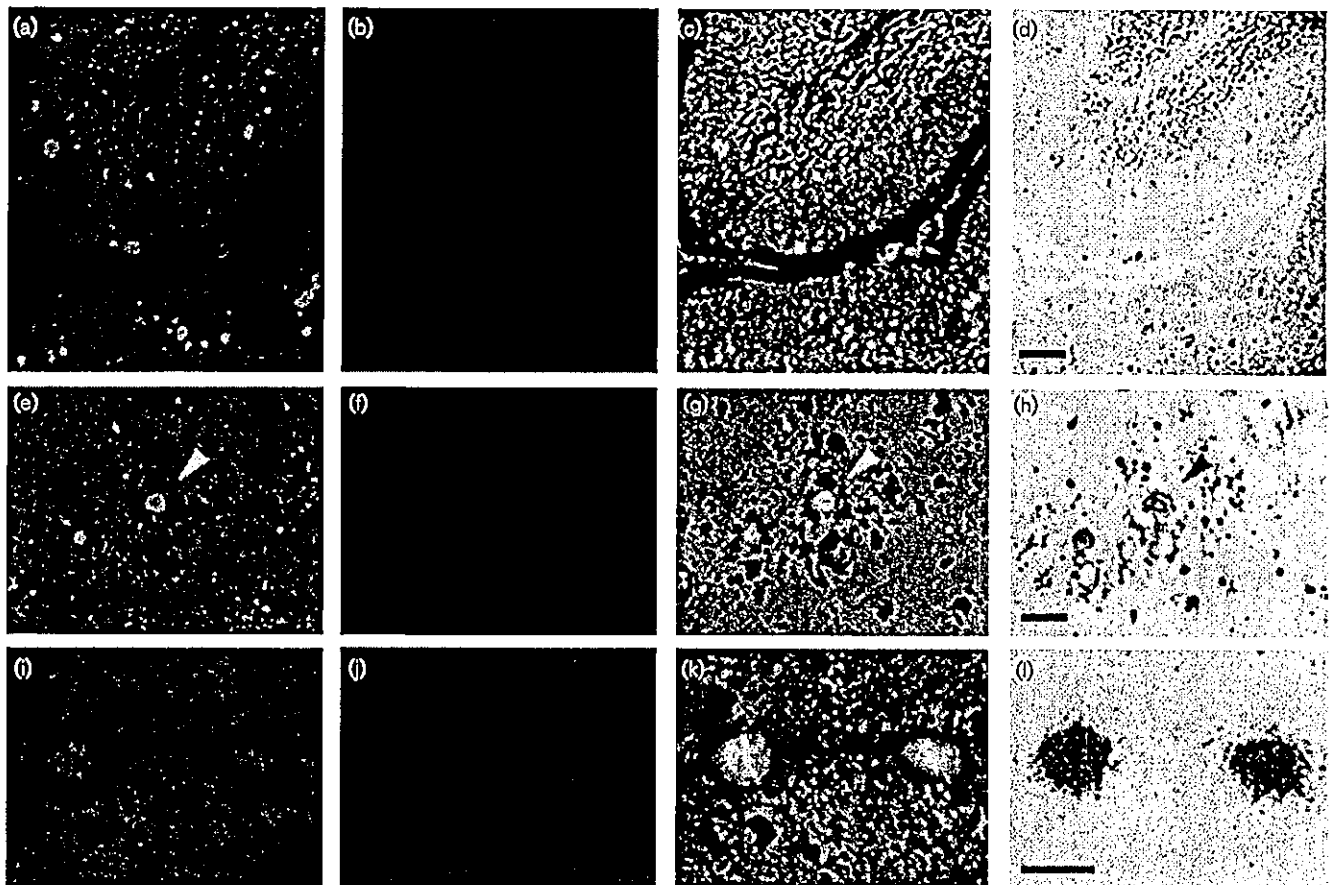


**Fig. 2.** Imaging of PrP aggregates in brains with TSE. PrP plaques were labelled with BTA-1 (a, e and i); no residual signal was seen after washing to remove BTA-1 (b, f and j). The plaques were then labelled with BSB (c, g and k), and subsequently immunostained for PrP (d, h and l). The first row shows a cerebellar section from a GSS case (a–d), the second shows a cerebral cortical section from a variant CJD case (e–h) and the third shows cerebral white matter section from a terminal Tg7 mouse (i–l). Only dense plaques are identified in the variant CJD section; the arrowheads point to the same PrP plaque. In the Tg7 section, PrP plaques in the cerebral white matter between the cortex and hippocampus were labelled. Bars, 100 (a–d) and 50 (e–l)  $\mu\text{m}$ .



sections from sporadic CJD cases, neither of the chemicals labelled synaptic-type PrP deposition (data not shown). Non-specific labelling was barely observed after rinsing off the excess chemicals. As reported in previous studies (Mathis *et al.*, 2002; Skovronsky *et al.*, 2000), both chemicals stained senile plaques in Alzheimer's brain, and neither displayed signals in control brain sections without amyloid (data not shown). Similar results to those observed in the human TSE brain sections were obtained from post-mortem brains of Tg7 mice infected with the 263K strain; both chemicals stained the plaque-type PrP deposition in the cerebral white matter between the cortex and hippocampus (Fig. 2i-l). There was no PrP immunohistochemical signal or fluorescent signal in the brains of uninfected Tg7 mice (data not shown).

Since both BTA-1 and BSB have been reported to cross the blood-brain barrier, we performed *in vivo* experiments using Tg7 mice in a later stage of 263K scrapie infection. A bolus injection of BTA-1 labelled PrP plaques in the white matter between the cortex and hippocampus of the affected brains (Fig. 3a and b). Faint cerebrovascular labelling was occasionally observed at 4 h after the injection, but not at 18 h or later. PrP imaging of BSB in the brain *in vivo* was almost as effective as that of BTA-1 (Fig. 3c), but non-specific cerebrovascular labelling was more evident. Images of PrP deposition labelled by BSB were not clearly distinguishable in the cerebrovascular images until 24 h post-administration, but background staining was not seen thereafter. The stability of the signals of PrP deposition was examined at various time-points, and both chemicals remained stably visible at 42 h post-injection. In particular, the BSB labelling signals were relatively stable and visible even at 54 h post-injection. There was no significant

labelling after an injection of either chemical to uninfected transgenic mice upon examination after sacrifice 24 h later, or after an injection of vehicle alone to infected mice (data not shown). Similar results were obtained for Tga20 mice infected with the RML strain, although labelled PrP plaques were less frequently observed (data not shown).

### Anti-prion activities *in vitro* and *in vivo*

The anti-prion activities of these chemicals were examined using three cell lines infected with different strains. Both BTA-1 and BSB inhibited PrP<sup>Sc</sup> formation in ScN2a cells in a dose-dependent manner (Fig. 4a). The concentrations giving 50% inhibition of PrP<sup>Sc</sup> formation in ScN2a cells relative to the untreated control (IC<sub>50</sub>) were 4 nM for BTA-1 and 1.4 μM for BSB. However, neither chemical was effective in the other cell lines (Fig. 4b and c). Treatment with vehicle (DMSO) alone showed no significant effects when compared with the untreated control. No apparent cell toxicity of the chemicals was observed up to 10 μM for BTA-1 and 100 μM for BSB. To examine the possibility of interference by the chemicals with immunodetection, BTA-1 or BSB at a concentration 10-fold higher than the IC<sub>50</sub>s were added to lysates of untreated ScN2a cells for 1 h prior to proteinase K digestion. After these treatments, the PrP signals were not affected (data not shown).

Since BSB was potent without significant toxicity at a high concentration of 100 μM in the cell cultures and remained stably bound to PrP aggregates in the affected brains for more than 2 days *in vivo*, we examined whether BSB could be an effective treatment for TSE in two different experimental animal models. As shown in Fig. 5, treatment with BSB at 1 mg prolonged the incubation period of Tga20 mice

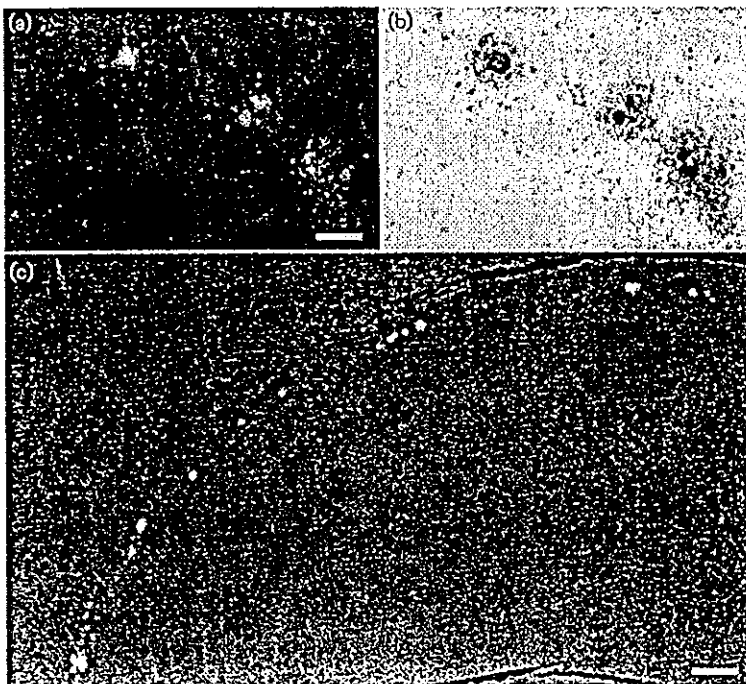


**Fig. 3.** *In vivo* imaging of PrP deposition in the brains of presymptomatic TSE-infected mice. An intravenous bolus injection of BTA-1 was given to Tg7 mice at 6 weeks post-infection, and they were sacrificed 24 h later. PrP plaques in the cerebral white matter between the cortex and hippocampus were detected under a fluorescent microscope (a), and then the brain section was immunostained for PrP (b). Similar results were observed with BSB (c, 24 h post-injection) and immunostaining for PrP (data not shown). Low magnification demonstrates PrP plaques in the cerebral white matter between the cortex and hippocampus were labelled with high specificity. All images are from coronal sections sited around one-third of the distance from the interaural line to the bregma line. Bars, 25 (a, b) and 100 (c) μm.

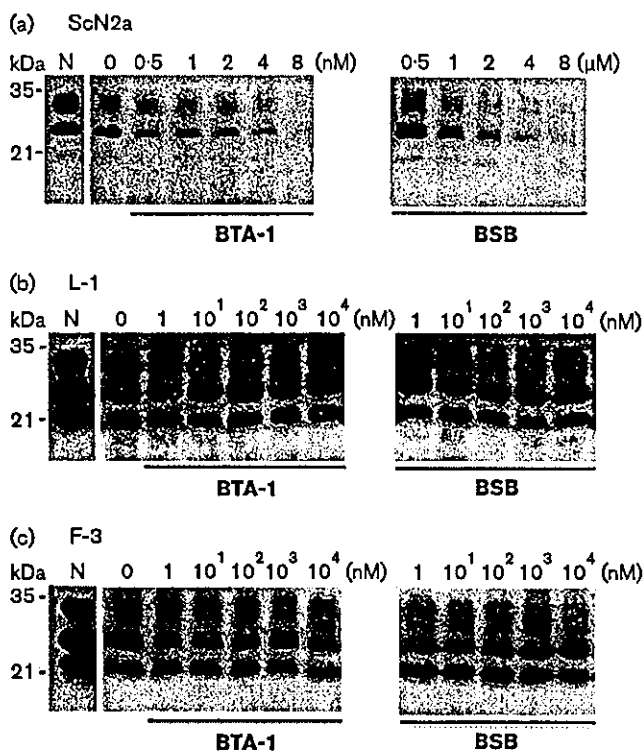


**Fig. 4.** Inhibition of PrP<sup>Sc</sup> formation in TSE-infected cells by BTA-1 or BSB. Various concentrations of each chemical were added to freshly passaged ScN2a cells in (a), L-1 cells in (b) and F-3 cells in (c), and the PrP<sup>Sc</sup> levels were analysed by Western blotting. Lanes: N, untreated cells; 0, cells treated with vehicle (DMSO) alone. Bars on the left indicate molecular mass markers at 35 and 21 kDa.

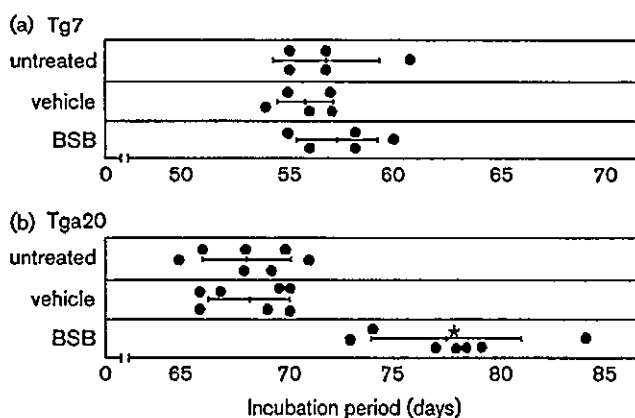


**Fig. 5.** Effects of BSB treatment on TSE-infected mice. BSB was administered to Tg7 mice infected with the 263K strain (a) and Tga20 mice infected with the RML strain (b). The treatment protocol is described in the text. Each closed circle represents an individual animal. Bars represent the mean and standard deviation of the incubation periods of each group. \* $P < 0.0001$  versus the other groups.

infected with the RML strain by 13.6% ( $77.6 \pm 3.6$  days in the BSB-treated group versus  $68.3 \pm 1.9$  days in the vehicle control), whereas no significant prolongation was observed in the same treatment for Tg7 mice infected with the 263K strain ( $57.4 \pm 1.9$  days in the BSB-treated group versus  $55.8 \pm 1.3$  days in the vehicle control). The dosage of BSB examined here corresponds to the concentration sufficient to detect PrP plaques *in vivo* as described above, and there were no apparent adverse effects of BSB. No significant differences in incubation times were observed between the untreated controls and the controls treated with vehicle (DMSO) alone ( $68.1 \pm 2.1$  days in the untreated control versus  $68.3 \pm 1.9$  days in the vehicle control in Tga20 mice;  $57.0 \pm 2.4$  days in the untreated control versus  $55.8 \pm 1.3$  days in the vehicle control in Tg7 mice).

## DISCUSSION

Both BTA-1 and BSB have been reported to be candidates for PET/SPECT tracers for the evaluation of Alzheimer's disease, and the results of this study have shown that they might also be useful for the evaluation of TSE with certain strains. However, the discrepancy in imaging between the plaque-type and the synaptic-type PrP deposition remains. A previous study demonstrated successful labelling of intracellular A $\beta$ (1–42) accumulation in living cells by BSB (Skovronsky *et al.*, 2000), but the same chemical showed no labelling of PrP<sup>Sc</sup> deposits in ScN2a cells (data not shown). These observations suggest that differences in the structures and/or the microenvironments of these PrP aggregates might account for the discrepancy. Further studies using more sensitive detection methods, such as the use of radiolabelling, might be helpful for evaluation.

Together with previous studies (Mathis *et al.*, 2002; Skovronsky *et al.*, 2000), the current study suggests that both BTA-1 and BSB label various amyloids including A $\beta$  aggregates and PrP aggregates, and are not disease specific. However, these chemicals can be still useful to evaluate amyloid aggregates because anatomical distributions of pathological deposition are quite different between different diseases. For example, A $\beta$  plaques are not, or seldom, observed in the cerebellum, while PrP amyloid plaques are predominantly observed there.

We also demonstrated therapeutic efficacies of these two chemicals. Congo red is well known to inhibit new formation of PrP<sup>Sc</sup> in ScN2a cells and prolongs the incubation period of infected animals when administered prophylactically (Caughey *et al.*, 1993; Ingrassio *et al.*, 1995). However, Congo red cannot be used as a therapeutic drug because of its inability to cross the blood–brain barrier and its carcinogenicity due to its benzidine structure. BSB, a Congo red analogue, can enter the brain and lacks the benzidine structure. Here BSB showed a low toxicity and was as potent as Congo red in a cellular model, and furthermore, BSB-treatment prolonged the incubation period of the Tga20-RML infected mouse model despite being introduced at a late stage of TSE infection.

There was a discrepancy in the efficacy of BSB between Tg7 mice infected with the 263K strain and Tga20 mice infected with the RML strain. This discrepancy *in vivo* is consistent with that found *in vitro*, since BSB was only effective in ScN2a cells, which are infected with the RML strain. There is a possibility that the differences in susceptibility to these chemicals among the three cell lines might be caused by the differences in the expression levels of normal PrP, because the expression levels of normal PrP in L-1 cells or F-3 cells are five times higher than that of ScN2a cells. However, the data showed that the two chemicals had no effect in either L-1 cells or F-3 cells, even at doses five times greater than the IC<sub>50</sub> in ScN2a cells. The findings suggest that the therapeutic efficacies of these chemicals are dependent on the TSE strain. In this study, we observed that the chemicals bound tightly to some kinds of PrP aggregates in the pathological sections of TSE, implying that a direct interaction with abnormal PrP molecules may play a role in the inhibition of PrP<sup>Sc</sup> formation. However, the mechanism of the strain-specific efficacies of these chemicals remains to be elucidated.

Together with previous reports (Caughey *et al.*, 1993; Ingrassio *et al.*, 1995; Supattapone *et al.*, 2002), the current study demonstrated that chemicals with a high affinity for amyloid could be candidates for inhibiting PrP<sup>Sc</sup> formation and increasing the life-span of TSE-infected animals. We tested this further by examining another chemical, 6-OH-BTA-1, which has recently been reported to facilitate PET studies of Alzheimer's disease (Engler *et al.*, 2002). We observed that this chemical inhibited PrP<sup>Sc</sup> formation in ScN2a cells with an IC<sub>50</sub> in the nanomolar order (data not shown), but *in vivo* studies remain to be performed.

In conclusion, BTA-1 and BSB, known as amyloid imaging probes, detected PrP deposition in the TSE brains both *in vitro* and *in vivo* and had anti-prion activities both *in vitro* and *in vivo*, although the efficacy depended upon the strain of TSE. These observations suggest that both could be lead chemicals not only for imaging probes, but also for therapeutic drugs for TSEs caused by certain strains.

## ACKNOWLEDGEMENTS

This study was supported by grants to K.D. from the Ministry of Health, Labour and Welfare (H13-kokoro-025) and the Ministry of Education, Culture, Sports, Science and Technology (13557118, 14021085), Japan. The authors thank Dr James W. Ironside of the CJD Surveillance Unit in Edinburgh University for the variant CJD specimens and Dojindo Laboratories, Kumamoto, Japan, for the BSB compound.

## REFERENCES

- Bacskai, B. J., Klunk, W. E., Mathis, C. A. & Hyman, B. T. (2002). Imaging amyloid- $\beta$  deposits *in vivo*. *J Cereb Blood Flow Metab* 22, 1035–1041.
- Caughey, B. & Raymond, G. J. (1993). Sulfated polyanion inhibition of scrapie-associated PrP accumulation in cultured cells. *J Virol* 67, 643–650.
- Caughey, B., Ernst, D. & Race, R. E. (1993). Congo red inhibition of scrapie agent replication. *J Virol* 67, 6270–6272.
- Demaerel, P., Baert, A. L., Vanopdenbosch, L., Robberecht, W. & Dom, R. (1997). Diffusion-weighted magnetic resonance imaging in Creutzfeldt–Jakob disease. *Lancet* 349, 847–848.
- Doh-ura, K., Mekada, E., Ogomori, K. & Iwaki, T. (2000). Enhanced CD9 expression in the mouse and human brains infected with transmissible spongiform encephalopathies. *J Neuropathol Exp Neurol* 59, 774–785.
- Engler, H., Nordberg, A., Blomqvist, G. & 11 other authors (2002). First human study with a benzothiazole amyloid-imaging agent in Alzheimer's disease and control subjects. *Neurobiol Aging* 23, S429.
- Fischer, M., Rulicke, T., Raeber, A., Sailer, A., Moser, M., Oesch, B., Brandner, S., Aguzzi, A. & Weissmann, C. (1996). Prion protein (PrP) with amino-proximal deletions restoring susceptibility of PrP knockout mice to scrapie. *EMBO J* 15, 1255–1264.
- Hamad, A., Hamad, A., Sokrab, T. E., Momeni, S. & Brown, P. (2001). Iatrogenic Creutzfeldt–Jakob disease at the millennium. *Neurology* 56, 987.
- Ingrassio, L., Ladogana, A. & Pocchiarl, M. (1995). Congo red prolongs the incubation period in scrapie-infected hamsters. *J Virol* 69, 506–508.
- Mathis, C. A., Bacskai, B. J., Kajdasz, S. T. & 8 other authors (2002). A lipophilic thioflavin-T derivative for positron emission tomography (PET) imaging of amyloid in brain. *Bioorg Med Chem Lett* 12, 295–298.
- Murakami-Kubo, I., Doh-Ura, K., Ishikawa, K., Kawatake, S., Sasaki, K., Kira, J., Ohta, S. & Iwaki, T. (2004). Quinoline derivatives are therapeutic candidates for transmissible spongiform encephalopathies. *J Virol* 78, 1281–1288.
- Murata, T., Shiga, Y., Higano, S., Takahashi, S. & Mugikura, S. (2002). Conspicuity and evolution of lesions in Creutzfeldt–Jakob disease at diffusion-weighted imaging. *Am J Neuroradiol* 23, 1164–1172.
- Nishida, N., Harris, D. A., Vilette, D., Laude, H., Frobert, Y., Grassi, J., Casanova, D., Milhavel, O. & Lehmann, S. (2000). Successful transmission of three mouse-adapted scrapie strains to murine neuroblastoma cell lines overexpressing wild-type mouse prion protein. *J Virol* 74, 320–325.
- Priola, S. A., Raines, A. & Caughey, W. S. (2000). Porphyrin and phthalocyanine antiscrapie compounds. *Science* 287, 1503–1506.
- Prusiner, S. B. (1991). Molecular biology of prion diseases. *Science* 252, 1515–1522.
- Race, R. E., Caughey, B., Graham, K., Ernst, D. & Chesebro, B. (1988). Analyses of frequency of infection, specific infectivity, and prion protein biosynthesis in scrapie-infected neuroblastoma cell clones. *J Virol* 62, 2845–2849.
- Race, R. E., Priola, S. A., Bessen, R. A., Ernst, D., Dockter, J., Rall, G. F., Mucke, L., Chesebro, B. & Oldstone, M. B. (1995). Neuron-specific expression of a hamster prion protein minigene in transgenic mice induces susceptibility to hamster scrapie agent. *Neuron* 15, 1183–1191.
- Skovronsky, D. M., Zhang, B., Kung, M. P., Kung, H. F., Trojanowski, J. Q. & Lee, V. M. (2000). *In vivo* detection of amyloid plaques in a mouse model of Alzheimer's disease. *Proc Natl Acad Sci U S A* 97, 7609–7614.
- Supattapone, S., Nishina, K. & Rees, J. R. (2002). Pharmacological approaches to prion research. *Biochem Pharmacol* 63, 1383–1388.
- Will, R. G., Ironside, J. W., Zeldler, M. & 7 other authors (1996). A new variant of Creutzfeldt–Jakob disease in the UK. *Lancet* 347, 921–925.
- Yokoyama, T., Kimura, K. M., Ushiki, Y., Yamada, S., Morooka, A., Nakashiba, T., Sassa, T. & Ithara, S. (2001). *In vivo* conversion of cellular prion protein to pathogenic isoforms, as monitored by conformation-specific antibodies. *J Biol Chem* 276, 11265–11271.

## Quinoline Derivatives Are Therapeutic Candidates for Transmissible Spongiform Encephalopathies

Ikuko Murakami-Kubo,<sup>1,2\*</sup> Katsumi Doh-ura,<sup>1\*</sup> Kensuke Ishikawa,<sup>1</sup> Satoshi Kawatake,<sup>1†</sup>  
Kensuke Sasaki,<sup>1</sup> Jun-ichi Kira,<sup>2</sup> Shigeru Ohta,<sup>3</sup> and Toru Iwaki<sup>1</sup>

*Departments of Neuropathology<sup>1</sup> and Neurology,<sup>2</sup> Graduate School of Medical Sciences, Kyushu University, Fukuoka 812-8582, and Department of Graduate School of Biomedical Science, Hiroshima University, Hiroshima 734-8551,<sup>3</sup> Japan*

Received 2 June 2003/Accepted 8 October 2003

We previously reported that quinacrine inhibited the formation of an abnormal prion protein (PrPres), a key molecule in the pathogenesis of transmissible spongiform encephalopathy, or prion disease, in scrapie-infected neuroblastoma cells. To elucidate the structural aspects of its inhibiting action, various chemicals with a quinoline ring were screened in the present study. Assays of the scrapie-infected neuroblastoma cells revealed that chemicals with a side chain containing a quinuclidine ring at the 4 position of a quinoline ring (represented by quinine) inhibited the PrPres formation at a 50% inhibitory dose ranging from  $10^{-1}$  to  $10^1$   $\mu$ M. On the other hand, chemicals with a side chain at the 2 position of a quinoline ring (represented by 2,2'-biquinoline) more effectively inhibited the PrPres formation at a 50% inhibitory dose ranging from  $10^{-3}$  to  $10^{-1}$   $\mu$ M. A metabolic labeling study revealed that the action of quinine or biquinoline was not due to any alteration in the biosynthesis or turnover of normal prion protein, whereas surface plasmon resonance analysis showed a strong binding affinity of biquinoline with a recombinant prion protein. *In vivo* studies revealed that 4-week intraventricular infusion of quinine or biquinoline was effective in prolonging the incubation period in experimental mouse models of intracerebral infection. The findings suggest that quinoline derivatives with a nitrogen-containing side chain have the potential of both inhibiting PrPres formation *in vitro* and prolonging the incubation period of infected animals. These chemicals are new candidates for therapeutic drugs for use in the treatment of transmissible spongiform encephalopathies.

Transmissible spongiform encephalopathies (TSEs), or prion diseases, are a group of fatal neurodegenerative disorders that include Creutzfeldt-Jakob disease and Gerstmann-Sträussler-Scheinker disease (GSS) in humans and scrapie, bovine spongiform encephalopathy, and chronic wasting disease in animals. These disorders are characterized by the accumulation of an abnormal isoform of prion protein (PrPres), which is high in beta-sheet content and resistant to digestion with proteases (15). Recent outbreaks in younger people of acquired forms of human TSEs, such as variant Creutzfeldt-Jakob disease (19) and iatrogenic Creutzfeldt-Jakob disease with cadaveric growth hormone or dura graft (4), are prompting the development of therapeutic interventions as well as early diagnostics.

One possible therapeutic strategy is to inhibit PrPres formation in the infected host. Doh-ura et al. first reported that cysteine protease inhibitors and lysomotropic agents inhibited PrPres formation in scrapie-infected neuroblastoma (ScNB) cells and that among them, quinacrine was one of the most

potent inhibitors (8). Another research group has also reported that quinacrine and its related tricyclic compounds are effective in inhibiting PrPres formation (11). Quinacrine is a synthesized chemical which has a quinoline ring in its structure. It is used as a substitute for quinine in the treatment of malaria. Accordingly, in this study we chose to focus on the quinoline derivatives to examine the structure-activity relationship involved in inhibiting PrPres formation as well as in prolonging the incubation time of infected animals.

### MATERIALS AND METHODS

**Chemicals and ScNB cells.** Chemicals were purchased from Sigma, Maybridge (Cornwall, United Kingdom), Peakdale (Derbyshire, United Kingdom), Specs (Rijswijk, The Netherlands), and Bionet (Cornwall, United Kingdom) and were dissolved in 100% dimethyl sulfoxide (DMSO) or 96% ethanol just before use. ScNB cells (16) were grown in six-well culture plates in Opti-MEM (Invitrogen) supplemented with 10% fetal bovine serum. Chemicals at various concentrations were added to the medium when 1/20 of the confluent cells were passed. The final concentration of either DMSO or ethanol in the medium was less than 0.2%. The cultures were allowed to grow to confluence for 4 days.

**Western blot analysis.** PrPres was analyzed as described previously (5) with slight modification. Briefly, the cells in confluency were rinsed with phosphate-buffered saline (PBS) and lysed with lysis buffer (0.5% sodium deoxycholate, 0.5% Nonidet P-40, PBS). After low-speed centrifugation, the supernatant was treated with 10  $\mu$ g of proteinase K/ml for 30 min at 37°C. Digestion was stopped with 0.5 mM phenylmethylsulfonyl fluoride, and the supernatant was centrifuged at 100,000  $\times$  g for 30 min at 4°C. Pellets were resuspended in 30  $\mu$ l of the sample buffer by sonication. After being boiled, the sample was separated by electrophoresis on a Tris-glycine-sodium dodecyl sulfate–15% polyacrylamide gel electrophoresis (SDS-PAGE) and then electroblotted onto a polyvinylidene difluoride membrane (Millipore). The membrane was incubated with PrP-2B, an anti-PrP polyclonal antibody, against a mouse-bamster PrP fragment (amino acids 89 to 103) and then with an alkaline phosphatase-conjugated goat anti-

\* Corresponding author. Mailing address for Ikuko Murakami-Kubo: Department of Neuropathology, Graduate School of Medical Sciences, Kyushu University, 3-1-1 Maidashi, Higashi-ku, Fukuoka 812-8582, Japan. Phone: 81-92-642-5537. Fax: 81-92-642-5540. E-mail: i-muraka@np.med.kyushu-u.ac.jp. Mailing address for Katsumi Doh-ura: Department of Prion Research, Tohoku University Graduate School of Medicine, 2-1 Seiryō-cho, Aoba-ku, Sendai 980-8575, Japan. Phone: 81-22-717-8232. Fax: 81-22-717-8148. E-mail: doh-ura@mail.tains.tohoku.ac.jp.

† Present address: Department of Prion Research, Tohoku University Graduate School of Medicine, Sendai 980-8575, Japan.

rabbit antibody (Promega). Signals were visualized with CDP-Star detection reagent (Amersham) and were densitometrically analyzed. Either the concentration of a chemical giving 50% inhibition of PrPres formation relative to the control 50% inhibitory concentration ( $IC_{50}$ ) or the maximal concentration of a chemical that does not affect the rate of cell growth to confluence (TC) was estimated from more than three independent experiments.

**Metabolic labeling study.** Metabolic labeling of prion protein was performed as described previously (5). Briefly, subconfluent ScNB cells in 25-cm<sup>2</sup> flasks were rinsed three times with PBS and preincubated at 37°C in 1.5 ml of methionine-free minimal essential medium with 1% dialyzed fetal bovine serum and 1  $\mu$ M quinine or 2,2'-biquinoline. After 60 min of preincubation, 125  $\mu$ Ci of <sup>35</sup>S-labeled methionine (Amersham) was added to each flask and incubated for 60 min. Then 10 ml of chase medium with 1  $\mu$ M quinine or biquinoline was added, and the incubation was continued for 18 min, 2 h, or 8 h. Cells were rinsed three times with PBS and lysed with lysis buffer. After low-speed centrifugation, an aliquot of the supernatant was electrophoresed for total protein analysis; the remainder was used for immunoprecipitation of total prion protein. For the detection of cell surface phosphatidylinositol-anchored prion protein, cells were incubated for 30 min in the chase medium with 1  $\mu$ M quinine or biquinoline after pulse labeling, rinsed three times with PBS, and then incubated with 1.33 U of phosphatidylinositol-specific phospholipase C (PIPLC)/ml in PBS at 37°C for 60 min. The soup was used for immunoprecipitation of cell-surface prion protein. Immunoprecipitation was performed with a PrP-2B antibody after whole proteins in the soup were precipitated with methanol and resuspended in detergent-lipid-protein complex solution.

**Surface plasmon resonance sensorgram study.** Interaction between prion protein and a chemical was analyzed using a BIAcore X systems. A recombinant murine prion protein fragment (amino acids 121 to 231) (PrP121-231) was immobilized on a sensor chip (CMS) according to the manufacturer's instructions. Each chemical was injected at a 100  $\mu$ M concentration in running buffer (2.5% DMSO in PBS) for 1 min at a flow rate of 20  $\mu$ l/min; then running buffer without a chemical was injected for 1 min at the same flow rate. Data were corrected by using a blank sensor chip as a control.

**In vivo study.** In vivo evaluation of the effectiveness of a chemical at prolonging the incubation times in infected animals was performed by using a mouse model of Tg7 (14, 17) or Tg20 (10), both of which have substantially shorter incubation periods than wild mice. Briefly, a 20- $\mu$ l aliquot of 1% 263K pathogen homogenate for Tg7 mice, or the same amount of aliquot of 1% Rocky Mountain Laboratory (RML) pathogen homogenate or Fukuoka-1 pathogen homogenate for Tg20 mice, was inoculated into the right parietal portion of the brain. A 4-week continuous intraventricular infusion of vehicle alone (25% DMSO) or of a chemical dissolved in 25% DMSO was initiated at day 10 or 35 in Tg7 mice or at day 14 or 49 in Tg20 mice by using an Alzet osmotic pump equipped with a brain infusion kit (Durect, Cupertino, Calif.). An intraventricular infusion cannula from the brain infusion kit was fitted into the left frontal portion of the brain.

The infusion initiation date was selected at an early stage of the infection (day 10 or 14), or at a late stage (day 35 or 49), when abnormal PrP deposition in the brain definitely appeared in the 263K-infected Tg7 or RML-infected Tg20 mice. However, day 49 postinoculation in the Fukuoka-1-infected Tg20 mice was not exactly at a late stage of the infection, and no information on when abnormal PrP deposition appeared in this model was available.

In some experiments, intraperitoneal administration of a chemical was provided by a single injection once a day for 5 days per week from day 10 or day 35 postintracerebral inoculation until death. The incubation period during which the animals were observed every day lasted from the time of intracerebral infection until the time of death. Five male mice (each weighing about 30 g) per group were used in the experiments. Animal handling and killing were in accordance with national prescribed guidelines, with ethical approval for the study granted by the Animal Experiment Committee of Kyushu University.

Mice which died within a few days due to operational procedures were accepted from the statistical analysis after pathological confirmation. Doses of less than 8 nmol of quinine/day were examined, because toxicity shortened life span at doses beyond 8 nmol/day. Biquinoline was examined at doses of less than 16 nmol/day, which provided no toxicity yet solubility in 25% DMSO.

**Immunohistochemistry.** An indirect immunoperoxidase method was applied as described previously (9) with slight modification. Briefly, brains were obtained postmortem and fixed in 10% buffered formalin for several weeks. The tissue was immersed in 98% formic acid for 1 h to reduce infectivity and then embedded in paraffin. The samples were cut into 5- $\mu$ m-thick sections, and then the sections were deparaffinized in xylene and hydrated using an ethanol gradient. The endogenous peroxidase activity was blocked with 0.3% H<sub>2</sub>O<sub>2</sub> in absolute methanol for 30 min at room temperature. After being rinsed with tap water, the

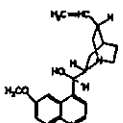
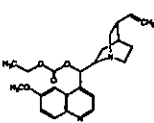
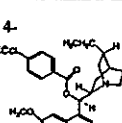
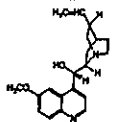
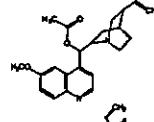
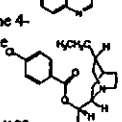
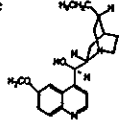
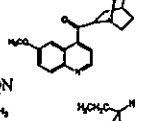
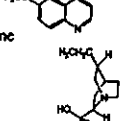
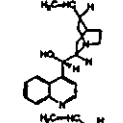
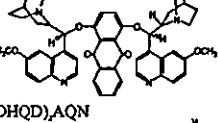
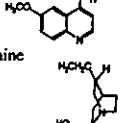
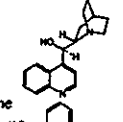
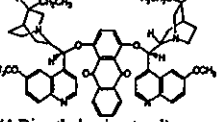
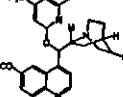
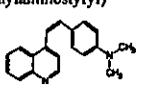
sections were treated with a hydrolytic autoclave (1 mM or 1.5 mM HCl, 121°C, 10 min) and washed in 50 mM Tris-HCl, pH 7.6, before being incubated with PrP-C polyclonal antibody (Immuno-Biological Laboratories, Gunma, Japan) (1:200) at 4°C overnight. The sections were then incubated with a horseradish peroxidase-conjugated secondary antibody (Vector Laboratories, Burlingame, Calif.) (1:200). The color reaction product was developed with 3,3'-diaminobenzidine tetrahydrochloride solution, and the sections were then counterstained with hematoxylin.

## RESULTS

**Screening of chemicals in vitro.** Clinically available drugs with a quinoline ring and their related chemicals were first screened for the inhibition of PrPres formation in ScNB cells. The antimalarial drug quinine and its related chemicals (such as quinidine, hydroquinine, cinchonine, cinchonidine, and hydroquinidine 4-methyl-2-quinolyl ether) were found to be effective (Table 1, left column). The  $IC_{50}$  doses of these chemicals ranged from 3 to 18  $\mu$ M, and the effective dose range between the  $IC_{50}$  and the TC was relatively narrow. Hydroquinidine 4-methyl-2-quinolyl ether, which has two quinoline rings, was slightly more effective than the chemicals with only one quinoline ring. Quinine-related chemicals with a carbonyl base located between a quinoline ring and a quinuclidine ring, such as MQAC (cinchonan-9-ol, 6'-methoxy-ethylcarbonate), MQAA (cinchonan-9-ol, 6'-methoxy-acetate), and MAM [(6-ethynyl-1-azabicyclo[2.2.2]oct-2yl) (6-methoxy-4-quinolinyl) methanone], were more effective, and their  $IC_{50}$  dose ranges were 0.45 to 0.9  $\mu$ M (Table 1, middle column). Chemicals with either the motif of quinine or that of quinidine on each lateral side of anthraquinone, (DHQ)<sub>2</sub>AQN (hydroquinine anthraquinone-1,4-diyl diether) and (DHQD)<sub>2</sub>AQN (hydroquinidine anthraquinone-1,4-diyl diether), were much more effective than those with only one motif, and their  $IC_{50}$  doses were 0.04 and 0.01  $\mu$ M, respectively. A chemical with a 4-dimethylaminoethyl moiety was also very effective; and its  $IC_{50}$  was 0.012  $\mu$ M. Except for this chemical, all of the effective chemicals shared a common structure composed of a quinoline ring plus a relative large side chain containing a quinuclidine ring at the 4 position of the quinoline ring. The chemicals listed in the right column of Table 1 also had this common structure, but they showed toxicity at a lower dose and were not effective within a nontoxic dose range.

Other quinoline chemicals unrelated to quinine were also screened. Chemicals with a side chain at the 2 position of a quinoline ring, such as 2,2'-biquinoline, inhibited PrPres formation at 0.003  $\mu$ M, the minimum  $IC_{50}$  dose (Fig. 1A), and this effectiveness was reduced by the replacement of the quinoline ring by a pyridine ring or a naphthyridine ring (Table 2, left column). The addition of a carboxyl moiety to both the 4 position and the 4' position of the quinoline ring abolished the inhibiting activity of biquinoline (Table 2, right column, top). QCQH (8-hydroxy-8-quinolinylhydrazone-2-quinolinecarboxaldehyde) and PCQH (2-quinolinylhydrazone-2-pyridinecarboxaldehyde) were also very effective in inhibiting PrPres formation at an  $IC_{50}$  dose of 0.0075 and 0.004  $\mu$ M, respectively. They shared a common structure with biquinoline respecting the arrangement of nitrogen atoms. DMEDAPQ (*N,N*-dimethyl-*N'*-[2-(4-pyridinyl)-4-quinolinyl]-1,2-ethanediamine) a chemical with a nitrogen-containing side chain at both the 2 position and the 4 position of a quinoline ring (thereby resem-

TABLE 1. Structure-activity relationship of quinine analogues on PrPres inhibition

Effective				Ineffective							
Chemical	Structure	IC <sub>50</sub> (μM) <sup>a</sup>	TC (μM) <sup>b</sup>	Chemical	Structure	IC <sub>50</sub> (μM) <sup>a</sup>	TC (μM) <sup>b</sup>	Chemical	Structure	IC <sub>50</sub> (μM) <sup>a</sup>	TC (μM) <sup>b</sup>
Quinine		6	50	MQAC		0.45	25	Hydroquinine 4-chlorobenzoate		-	5
Quinidine		3	>50	MQAA		0.5	>50	Hydroquinidine 4-chlorobenzoate		-	>5
Hydroquinine		12.5	50	MAM		0.9	>50	Hydroquinidine		-	2.5
Cinchonine		6	25	(DHQ) <sub>2</sub> AQN		0.04	5	Hydrocinchonine		-	25
Cinchonidine		18	50	(DHQD) <sub>2</sub> AQN		0.01	5				
Hydroquinidine 4-methyl-2-quinolyli ether		3.5	>5	4-(4-Dimethylaminostyryl) quinoline		0.012	10				

<sup>a</sup> IC<sub>50</sub>, approximate concentration of a chemical giving 50% inhibition of PrPres formation relative to the control.  
<sup>b</sup> TC, approximate maximal concentration of a chemical that does not affect the rate of cell growth to confluence.

bling quinine rather than biquinoline in terms of the arrangement of nitrogen atoms), was less effective than biquinoline, and its IC<sub>50</sub> dose was 0.5 μM.

Chemicals containing a quinoline ring without a large side chain were also examined. They included quinoline hydrochloride, 8-hydroxyquinoline, 2,8-quinolinediol, 8-acetoxyquinoline, and CHIQ (5-chloro-7-iodo-8-quinolinol). All of them, with the exception of 2,8-quinolinediol, were ineffective at inhibiting PrPres within a nontoxic dose range (Table 2, right column). Quinolinediol showed an IC<sub>50</sub> dose of 8 μM, which was much higher than those of other chemicals with a side chain at the 2 position of a quinoline ring (Table 2, left column, bottom).

**Mechanism of inhibition of PrPres formation.** Because quinine and biquinoline represented the effective chemicals found here, we focused on these chemicals and studied the mechanism behind their action. After ScNB cells had been treated with different concentrations of quinine or biquinoline for 4 days, and then left without treatment for an additional 10 or 17 days, PrPres signals did not reappear even 17 days after discontinuation of the chemical treatment (Fig. 1B [for biquinoline] and data not shown [for quinine]). Thus, treatment with the chemicals permanently cured the cells of the accumulation of PrPres.

Because phospholipase-sensitive cell surface PrP (PrP<sup>sen</sup>) is

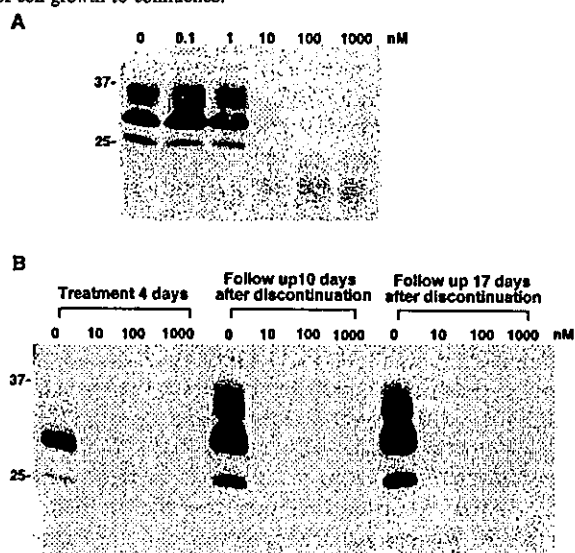


FIG. 1. Inhibition of PrPres accumulation in ScNB cells grown with 2,2'-biquinoline (A) and lack of restoration of PrPres formation in ScNB cells treated once with biquinoline (B). (A) Biquinoline was added at designated concentrations to the medium when the cells were passed, and the culture was allowed to grow to confluence. Then, PrPres in the cells was analyzed by immunoblotting. (B) ScNB cells were treated with 10, 100, or 1,000 nM biquinoline for 4 days. The medium was replaced by fresh medium, and the cells were left without treatment for an additional 10 or 17 days. Then PrPres levels were assayed. Molecular size markers (in kilodaltons) are indicated.

TABLE 2. Structure-activity relationship of biquinoline analogues on PrPres inhibition

Effective				Ineffective			
Chemical	Structure	IC <sub>50</sub> (μM) <sup>a</sup>	TC (μM) <sup>b</sup>	Chemical	Structure	IC <sub>50</sub> (μM) <sup>a</sup>	TC (μM) <sup>b</sup>
2,2'-Biquinoline		0.003	>10	BQDA		-	>100
2-(2-Pyridinyl)quinoline		0.11	50	Quinoline hydrochloride		-	>25
2,2'-Bi(1,8-naphthyridine)		38	>100	8-Hydroxyquinoline		-	1
2-(2-Pyridinyl)-1,8-naphthyridine		12	200	8-Acetoxyquinoline		-	2.5
QCQH		0.0075	2.5	CHIQ		-	>5
PCQH		0.004	1				
DMEDAPQ		0.5	50				
2,8-Quinolinediol		8	>50				

<sup>a</sup> IC<sub>50</sub>, approximate concentration of a chemical giving 50% inhibition of PrPres formation relative to the control.

<sup>b</sup> TC, approximate maximal concentration of a chemical that does not affect the rate of cell growth to confluence.

the precursor of PrPres, it is possible that the inhibition of PrPres accumulation by these chemicals was due to an indirect effect on PrPsen metabolism or turnover. However, biquinoline showed no effects on the metabolic labeling of cellular proteins or on the biosynthesis and turnover of PrPsen (Fig. 2A, B, and C).

Surface plasmon resonance analysis showed that the interaction of biquinoline with recombinant PrP121-231 occurred very slowly and failed to reach saturation even after 1 min. During the dissociation phase, furthermore, complete dissociation did not occur (Fig. 2D). On the other hand, the interaction of quinine or quinacrine occurred very quickly, reaching saturation within several seconds, and dissociation was completely over within seconds.

From observations of the structure of the effective chemicals, it was predicted that they might exert their inhibiting action through some mechanism which involved chelating metals. Thus, quinine and biquinoline were preincubated (before being added to the ScNB culture medium) with an equivalent dose of, a 10-times-higher dose of, or a 100-times-higher dose of various metal ions, including copper, zinc, manganese, iron, cobalt, and aluminum ions. The results showed no change in the inhibiting activities of the chemicals (data not shown).

**In vivo study.** To examine whether these chemicals could be effective in improving the prognosis *in vivo*, quinine or biquinoline was continuously administered intraventricularly in animal

models which had been intracerebrally infected with three different TSE pathogen strains, comprising 263K scrapie agent, RML scrapie agent, and Fukuoka-1 GSS agent. Quinine administration from an early stage of infection prolonged the incubation period by 13.6% (days 47 to 53.4) at 0.64 nmol/day in 263K-infected mice (Fig. 3A), by 10.8% (days 68.6 to 76) at 1.6 nmol/day in RML-infected mice (Fig. 3B), and by 12.8% (days 104.2 to 117.5) at 0.64 nmol/day in Fukuoka-1-infected mice (Fig. 3C). The effect of quinine administration from a late stage of infection was clearly demonstrated in 263K-infected mice, resulting in 36% (days 47 to 63) prolongation of the incubation period at 1.6 nmol/day (Fig. 3A), with some of the RML-infected mice displaying a tendency to survive much longer than the control at 0.64 nmol/day (Fig. 3B). On the other hand, the effect of biquinoline administration was examined only in 263K-infected mice; it demonstrated 10.8% (days 49 to 54.3) prolongation of the incubation period in the group receiving 1.6 nmol/day at an early stage of infection, but no significant effects were observed in the groups which received it at a late stage (Fig. 3D). Intraperitoneal administration of biquinoline was also performed in 263K-infected mice, and this resulted in 7.7% (days 49 to 52.8) prolongation of the incubation period in the group receiving 0.39 mmol/day from an early stage of infection.

Postmortem histopathological examination of the brains treated with quinine or biquinoline was performed to see

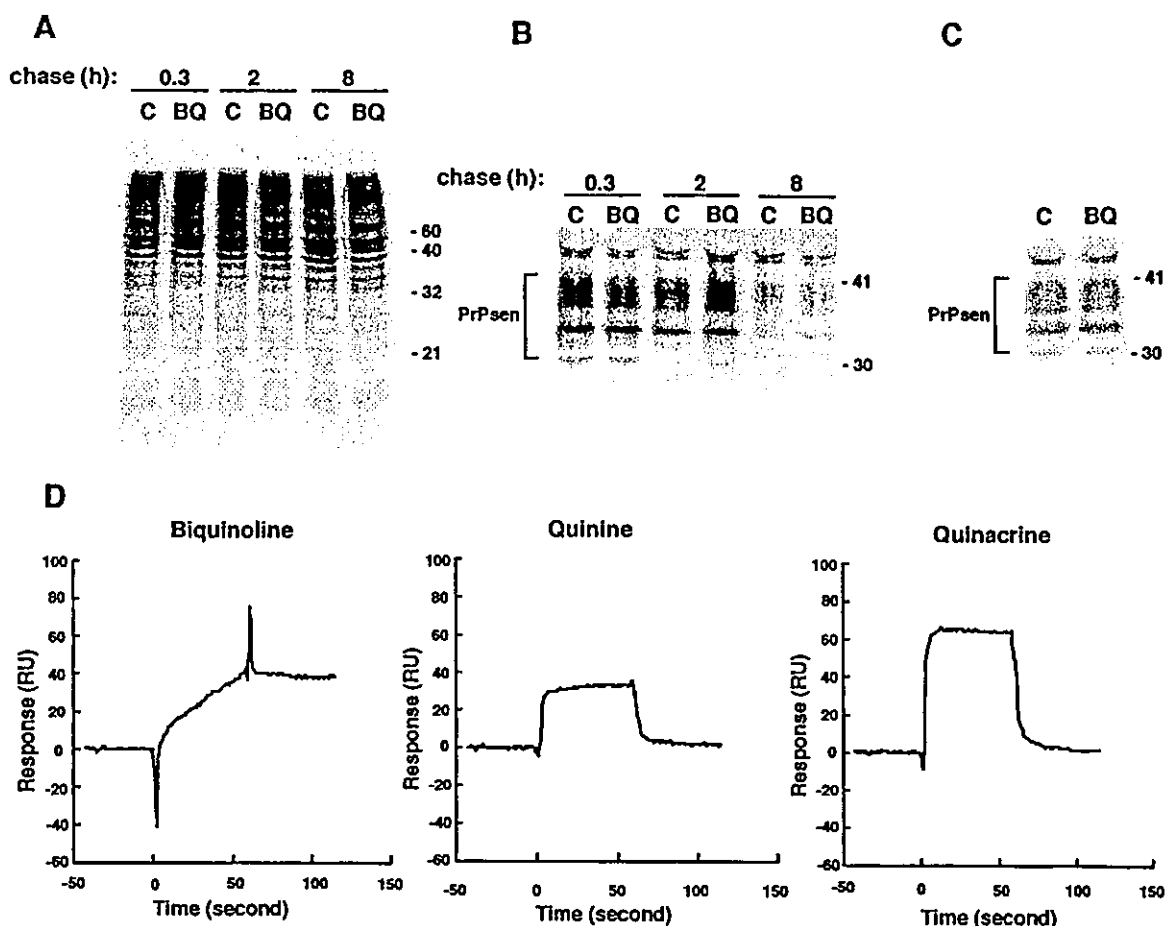


FIG. 2. Lack of effect of the presence of biquinoline on the metabolic labeling of total protein (A), total PrPsen (B), and PIPLC-sensitive, cell surface PrPsen (C). (D) Direct interaction of biquinoline with recombinant PrP121-231 analyzed using a surface plasmon resonance sensorgram. (A) Control ScNB cells (lanes C) and biquinoline-treated cells (lanes BQ) were pulse labeled and then incubated in chase medium for the indicated chase time. The total lysate proteins were methanol precipitated from the detergent lysates of the cells and analyzed by SDS-PAGE. Equal flask equivalents were loaded onto all lanes in each panel. Molecular size markers (in kilodaltons) are indicated. (B) PrPsen was isolated from the total lysate proteins by immunoprecipitation and analyzed by SDS-PAGE. (C) PrPsen was immunoprecipitated from the cell soup treated with PIPLC. Biquinoline at  $1 \mu\text{M}$  was included in all media, starting with the preincubation, except in the case of the control cells. (D) Interaction between a PrP121-231 fragment and a chemical was analyzed using a BiAcCore system. A recombinant murine PrP121-231 fragment was immobilized on a CM5 sensor chip; biquinoline, quinine, or quinacrine (at  $100 \mu\text{M}$  in buffer solution) was injected for 1 min at a flow rate of  $20 \mu\text{l}/\text{min}$  for the association, and then the buffer solution without a chemical was injected at the same flow rate for the dissociation.

whether there was any modification in abnormal PrP deposition patterns following treatment. Those mice with prolonged incubation periods had a tendency to show less PrP deposition in the white matter between the cerebral cortex and the hippocampus of the brain hemisphere implanted with an intraventricular cannula, although they showed no apparent alteration in PrP deposition patterns in the bilateral thalamus or hypothalamus (Fig. 4).

#### DISCUSSION

In the studies reported here, we were able to identify quinoline derivatives that inhibited PrPres accumulation in ScNB cells. The commonly shared structure in these chemicals was a quinoline ring bound at its 2 or 4 position with a side chain containing a nitrogen atom, which was located at a particular distance from a nitrogen atom in the ring. Chemicals with a

side chain at the 2 position of a quinoline ring were more effective than those with a side chain at the 4 position. Replacement of a quinoline ring with a pyridine ring or a naphthyridine ring resulted in a weaker inhibiting activity, while modification of biquinoline by a moiety that caused less flexibility in the hinge portion between the quinoline rings completely suppressed the inhibiting activity. These findings suggest that a certain proper alignment of two nitrogens, one in a quinoline ring and the other in a side chain, might be important with regard to inhibiting activity.

As for the inhibiting mechanism of these chemicals, the representative chemicals, quinine and biquinoline, demonstrated no alteration either in the protein biosynthesis in general or in the metabolic labeling and turnover of PrPsen in particular. However, biquinoline showed a very strong binding affinity with recombinant PrP121-231 in the Biacore study. Thus, some of the chemicals, including biquinoline, may inhibit



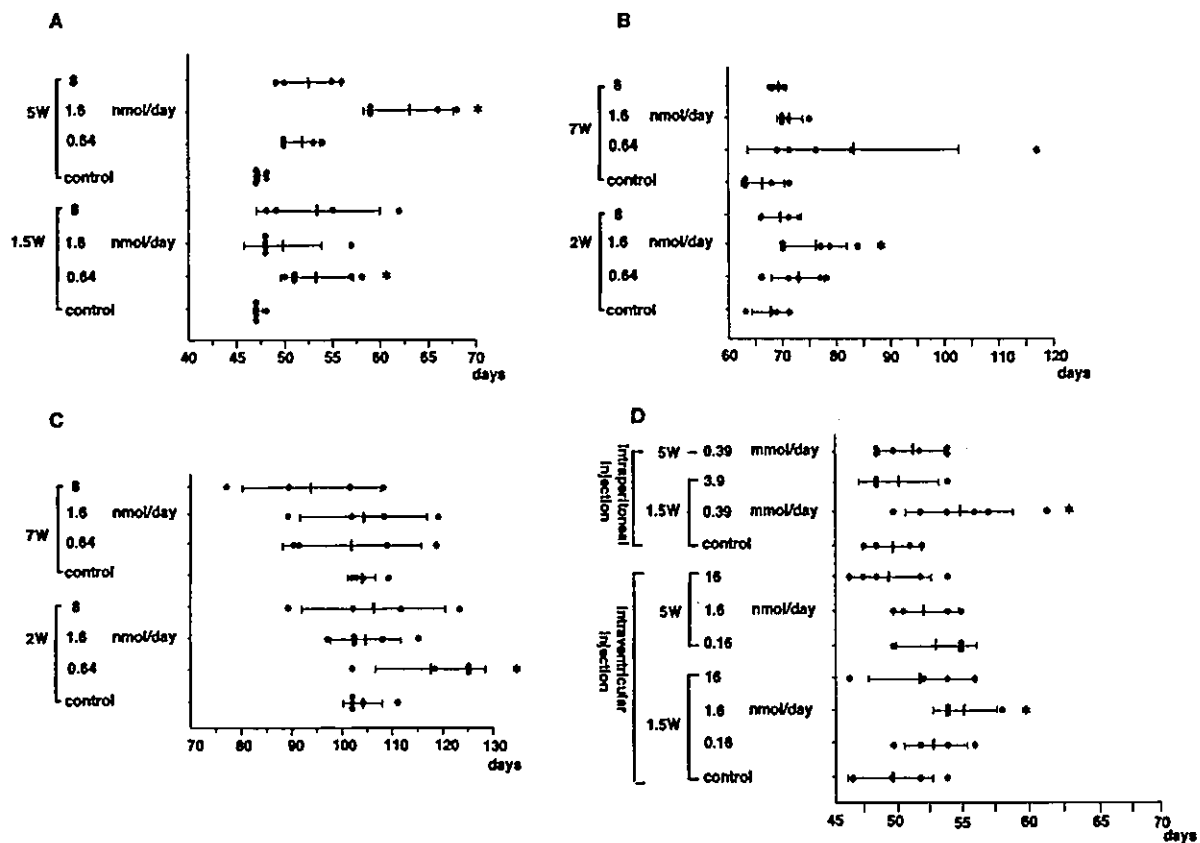


FIG. 3. Prolongation of incubation times in intracerebrally TSE-infected mice treated with quinine or biquinoline. (A) Tg7 mice infected with 263K agent strain and intraventricularly treated with quinine; (B) Tg20 mice infected with RML agent strain and intraventricularly treated with quinine; (C) Tg20 mice infected with Fukuoka-1 agent strain and intraventricularly treated with quinine; (D) Tg7 mice infected with 263K agent strain and intraperitoneally or intraventricularly treated with biquinoline. A 4-week continuous intraventricular infusion of a chemical was initiated by using an osmotic pump at day 10 (1.5W) or day 35 (5W) post-intracerebral inoculation in Tg7 mice or at day 14 (2W) or day 49 (7W) in Tg20 mice. For intraperitoneal treatment, injection of a chemical in Tg7 mice was performed intraperitoneally once a day for 5 days per week from day 10 (1.5W) or day 35 (5W) until the death of the mouse. Each closed circle represents the incubation time of an individual mouse. Each solid line and bar represent the average and standard deviation of the incubation times of each group. The star indicates groups with results with  $P < 0.05$  compared to the results seen with the vehicle control. Each of the experiments was performed independently using different lots of the pathogen homogenate; thus, there was some variation in the data shown in panels A and D even for the same vehicle control.

the conversion of PrPsen to PrPres through direct interaction with PrPsen molecules. Since biquinoline ( $IC_{50}$  dose, 0.003  $\mu$ M) was much more effective than quinine (3  $\mu$ M) or quina-crine (at a concentration of 0.4  $\mu$ M [8] or 0.3  $\mu$ M [11]) in ScNB cells, the binding affinity of the PrP fragment (which was much stronger with biquinoline than with quinine or quina-crine) would appear to be clearly correlated with the inhibiting activity of PrPres formation *in vitro*. The potential binding site(s) of these chemicals in PrPsen molecules remains to be determined.

On the other hand, the involvement of chelating metal(s) in their inhibiting activity (as determined on the basis of the structure of the chemicals which were found to be effective in this study) was predicted. PrPsen is known to bind copper at its N-terminal octameric repeat region (3, 13, 18), and it is suggested that interaction between PrPres and copper stabilizes PrPres conformation (12). Manganese also binds PrP molecules instead of copper and increases proteinase K resistance and beta-sheet content (2). However, our observation suggests

that the chelating mechanism seems unlikely to be involved in the inhibiting action of the chemicals found here.

Among the chemicals tested here, CHIQ is an antibiotic (called clioquinol) and a Cu/Zn-selective chelator known to be effective in decreasing beta-amyloid deposits in Alzheimer's disease (6). However, in this study, CHIQ and its related compounds, quinoline hydrochloride, 8-hydroxyquinoline, and 8-acetoxyquinoline, did not inhibit PrPres formation in ScNB cells. These findings also suggest that chelating drugs which are effective in inhibiting beta-amyloid formation are not necessarily effective at inhibiting PrPres formation.

The *in vivo* study revealed that the chemicals with a quinoline ring were effective not only in inhibiting PrPres formation *in vitro* but also in prolonging incubation times of intracerebrally infected animals. The greatest effectiveness was obtained by intraventricular administration of quinine at 1.6 nmol/day, which prolonged the incubation time by 36% in 263K-infected mice (compared to the results seen with the control) when initiated at a late stage of infection. Quinine was also effective

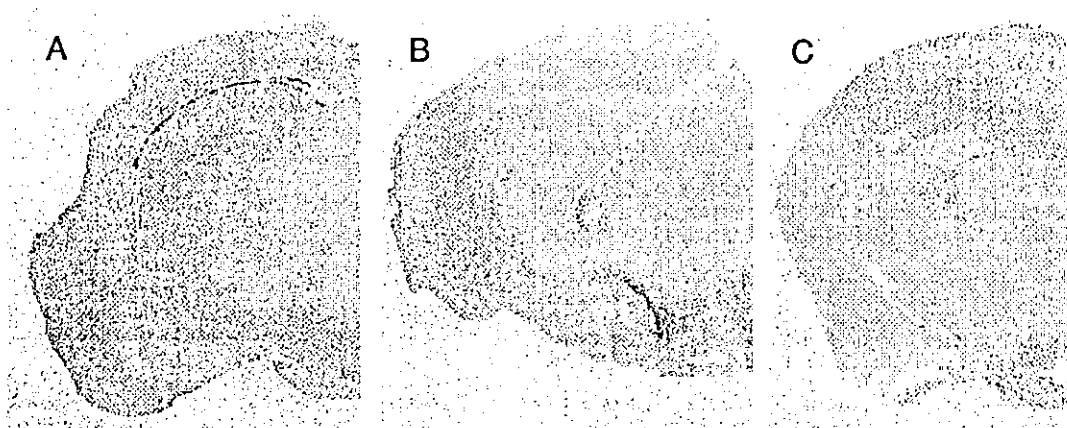


FIG. 4. Effects of intraventricular treatment with quinine or biquinoline on abnormal PrP deposition in the brain of intracerebrally 263K-infected Tg7 mice. The results for brain treated from day 10 postinfection for 4 weeks with vehicle (25% DMSO) alone (A), 0.64 nmol of quinine/day (B), or 1.6 nmol of biquinoline/day (C) are shown. Immunohistochemistry for abnormal PrP deposition was performed in the brains obtained postmortem from the longest-surviving members in each group, and representative examples of the brain hemisphere at the chemical injection side are shown.

in prolonging incubation times of the mice inoculated with different pathogen strains such as RML scrapie agent and Fukuoka-1 GSS agent. These findings indicate that application of quinine, an antimalarial drug, to humans infected with other TSE agents could be judicious.

Recently two research groups have reported that quinacrine is not effective in prolonging incubation times of intracerebrally infected TSE animals (1, 7). Our findings regarding quinine, which is a quinacrine-related chemical, appear to be inconsistent with their findings about quinacrine. However, differences in the structures of the chemicals and in the administration routes, doses, and durations as well as experimental models might have caused this gap but it remains to be elucidated.

Biquinoline was 1,000 times more effective than quinine in inhibiting PrPres formation *in vitro* with respect to the  $IC_{50}$  value, but when initiated from an early stage with intraventricular injections of 1.6 nmol/day or intraperitoneal injections of 0.39 mmol/day, its effectiveness in prolonging incubation times *in vivo* was clear, albeit marginal. The stability of chemicals and accessibility to targets *in vivo* might be different between these chemicals, and the reason for the gap between inhibiting activity *in vitro* and therapeutic activity *in vivo* remains to be found.

In investigations of the immunohistochemistry of the post-mortem materials, abnormal PrP deposition in the white matter adjacent to the ventricle (where a chemical was injected continuously) was less evident in the mice treated with quinine or biquinoline from an early stage than in the control, although abnormal PrP deposition in the thalamus and hypothalamus was demonstrated in a fashion similar to that seen in the control. This would seem to imply that following treatment with a chemical, prolongation of incubation times in mice treated with the chemical might be associated with a reduction in abnormal PrP deposition in the brain.

In conclusion, we have demonstrated that quinoline derivatives with a relatively large side chain with a nitrogen are able to inhibit PrPres accumulation in ScNB cells and can prolong

the incubation periods of infected mice. The inhibition was not caused by interference in the biosynthesis or turnover of PrPsen or by the chelation of metals. Some of the chemicals, including quinine, are already in clinical use and are known to pass the blood-brain barrier. Thus, these drugs might be immediately available for clinical trials in investigations of the treatment of human TSEs.

#### ACKNOWLEDGMENTS

This study was supported by grants to K.D. from the Ministry of Health, Labor and Welfare (H13-kokoro-025) and from the Ministry of Education, Culture, Sports, Science and Technology (13557118, 14021085), Japan.

We thank B. Chesebro and R. Race in the Rocky Mountain Laboratories, NIAID for providing Tg7 mice, C. Weissmann in the Imperial College School of Medicine at St. Mary's, United Kingdom for Tg20 mice, and S. Katamine and S. Sakaguchi in Nagasaki University, Nagasaki, Japan, for PrP121-231. We also thank N. Suzuki in Daiichi Pharmaceuticals, Tokyo, Japan, for screening the chemical database.

#### REFERENCES

1. Barret, A., F. Tagliavini, G. Forloni, C. Bate, M. Salmons, L. Colombo, A. De Luigi, L. Limido, S. Suardi, G. Rossi, F. Auvre, K. T. Adjou, N. Sales, A. Williams, C. Lasmezas, and J. P. Deslys. 2003. Evaluation of quinacrine treatment for prion diseases. *J. Virol.* 77:8462-8469.
2. Brown, D. R., F. Hafiz, L. L. Glasssmith, B. S. Wong, I. M. Jones, C. Clive, and S. J. Haswell. 2000. Consequences of manganese replacement of copper for prion protein function and proteinase resistance. *EMBO J.* 19:1180-1186.
3. Brown, D. R., K. Qin, J. W. Herms, A. Madlung, J. Manson, R. Strome, P. E. Fraser, T. Kruck, A. von Bohlen, W. Schulz-Schaeffer, A. Giese, D. Westaway, and H. Kretzschmar. 1997. The cellular prion protein binds copper *in vivo*. *Nature* 390:684-687.
4. Brown, P., M. Preece, J. P. Brandel, T. Sato, L. McShane, I. Zerr, A. Fletcher, R. G. Will, M. Pocchiari, N. R. Cashman, J. H. d'Aignaux, L. Cervenakova, J. Fradkin, L. B. Schonberger, and S. J. Collins. 2000. Iatrogenic Creutzfeldt-Jakob disease at the millennium. *Neurology* 55:1075-1081.
5. Caughey, B., and G. J. Raymond. 1993. Sulfated polyanion inhibition of scrapie-associated PrP accumulation in cultured cells. *J. Virol.* 67:643-650.
6. Cherny, R. A., C. S. Atwood, M. E. Xilinas, D. N. Gray, W. D. Jones, C. A. McLean, K. J. Barnham, I. Volitakis, F. W. Fraser, Y. Kim, X. Huang, L. E. Goldstein, R. D. Moir, J. T. Lim, K. Beyreuther, H. Zheng, R. E. Tanzi, C. L. Masters, and A. I. Bush. 2001. Treatment with a copper-zinc chelator markedly and rapidly inhibits beta-amyloid accumulation in Alzheimer's disease transgenic mice. *Neuron* 30:665-676.
7. Collins, S. J., V. Lewis, M. Brazier, A. F. Hill, A. Fletcher, and C. L. Masters.

2002. Quinacrine does not prolong survival in a murine Creutzfeldt-Jakob disease model. *Ann. Neurol.* 52:503–506.
8. Doh-ura, K., T. Iwaki, and B. Caughey. 2000. Lysosomotropic agents and cysteine protease inhibitors inhibit scrapie-associated prion protein accumulation. *J. Virol.* 74:4894–4897.
9. Doh-ura, K., E. Mekada, K. Ogomori, and T. Iwaki. 2000. Enhanced CD9 expression in the mouse and human brains infected with transmissible spongiform encephalopathies. *J. Neuropathol. Exp. Neurol.* 59:774–785.
10. Fischer, M., T. Rulicke, A. Raeber, A. Sailer, M. Moser, B. Oesch, S. Brandner, A. Aguzzi, and C. Weissmann. 1996. Prion protein (PrP) with amino-proximal deletions restoring susceptibility of PrP knockout mice to scrapie. *EMBO J.* 15:1255–1264.
11. Korth, C., B. C. May, F. E. Cohen, and S. B. Prusiner. 2001. Acridine and phenothiazine derivatives as pharmacotherapeutics for prion disease. *Proc. Natl. Acad. Sci. USA* 98:9836–9841.
12. McKenzie, D., J. Bartz, J. Mirwald, D. Olander, R. Marsh, and J. Aiken. 1998. Reversibility of scrapie inactivation is enhanced by copper. *J. Biol. Chem.* 273:25545–25547.
13. Miura, T., A. Hori-i, H. Mototani, and H. Takeuchi. 1999. Raman spectroscopic study on the copper(II) binding mode of prion octapeptide and its pH dependence. *Biochemistry* 38:11560–11569.
14. Priola, S. A., A. Raines, and W. S. Caughey. 2000. Porphyrin and phthalocyanine antiscrapie compounds. *Science* 287:1503–1506.
15. Prusiner, S. B. 1991. Molecular biology of prion diseases. *Science* 252:1515–1522.
16. Race, R. E., B. Caughey, K. Graham, D. Ernst, and B. Chesebro. 1988. Analyses of frequency of infection, specific infectivity, and prion protein biosynthesis in scrapie-infected neuroblastoma cell clones. *J. Virol.* 62:2845–2849.
17. Race, R. E., S. A. Priola, R. A. Bessen, D. Ernst, J. Dockter, G. F. Rall, L. Mucke, B. Chesebro, and M. B. Oldstone. 1995. Neuron-specific expression of a hamster prion protein minigene in transgenic mice induces susceptibility to hamster scrapie agent. *Neuron* 15:1183–1191.
18. Viles, J. H., F. E. Cohen, S. B. Prusiner, D. B. Goodin, P. E. Wright, and H. J. Dyson. 1999. Copper binding to the prion protein: structural implications of four identical cooperative binding sites. *Proc. Natl. Acad. Sci. USA* 96:2042–2047.
19. Will, R. G., J. W. Ironside, M. Zeidler, S. N. Cousens, K. Estibeiro, A. Alperovitch, S. Poser, M. Pocchiari, A. Hofman, and P. G. Smith. 1996. A new variant of Creutzfeldt-Jakob disease in the UK. *Lancet* 347:921–925.

# Clinical features of Creutzfeldt–Jakob disease with V180I mutation

K. Jin, MD; Y. Shiga, MD, PhD; S. Shibuya, MD, PhD; K. Chida, MD, PhD; Y. Sato, MD, PhD; H. Konno, MD, PhD; K. Doh-ura, MD, PhD; T. Kitamoto, MD, PhD; and Y. Itoyama, MD, PhD

**Abstract**—The authors describe the clinical features of Creutzfeldt–Jakob disease (CJD) with the causative point mutation at codon 180. The symptoms never started with visual or cerebellar involvement. The patients showed slower progression of the disease compared with sporadic CJD. They never showed periodic sharp and wave complexes in EEG. MRI demonstrated remarkable high-intensity areas with swelling in the cerebral cortex except for the medial occipital and cerebellar cortices. These characteristic MRI findings are an important clue for an accurate premortem diagnosis.

NEUROLOGY 2004;62:502–505

Approximately 10 to 15% of all Creutzfeldt–Jakob disease (CJD) cases are estimated to be familial.<sup>1</sup> Some of them are sporadic cases with no relevant family history because of incomplete genetic penetrance and the misdiagnosis of other affected family members. The clinical features depend on the genetic mutations. However, most patients demonstrate periodic sharp and wave complexes (PSWC) in EEG, an accepted diagnostic marker for CJD.

CJD with a causative point mutation of valine to isoleucine at codon 180 (V180I)<sup>2–5</sup> is a type of familial CJD with no relevant family history. In case reports, the clinical features of CJD with V180I (CJD180) were different from those of sporadic CJD (sCJD). Therefore, the premortem clinical diagnosis was difficult, and the cases had been misdiagnosed as neurodegenerative disorders with dementia. We herein report the clinical features and characteristic MRI findings of five original cases of CJD180 together with a review of four reported cases.

**Patients and methods.** *Patients.* Nine patients including our five original patients and four other previously reported pathologically verified patients<sup>2–5</sup> were studied retrospectively. The clinical features of these patients are shown in table 1. The previously reported case with a double mutation at codon 180 and codon 232 of the PRNP was excluded from this study because the codon 232 mutation might influence the clinical course.<sup>6</sup> All nine had neither family history of dementia nor obvious iatrogenic exposure. Their PRNP analyses at codon 129 revealed that four had methionine homozygosity (MM129) and five had methionine/valine heterozygosity (MV129), in which the V180I mutation and valine at codon 129 were on different alleles.

The common histopathologic findings in the five pathologically verified patients were evident spongiform changes in all layers of the cerebral cortex with less prominent neuronal loss and gliosis without Kuru plaque. Immunohistochemical analysis showed

weak prion protein staining of the synaptic type in three of three patients examined.<sup>2,4,5</sup>

**Methods.** We compared the clinical features, laboratory findings, and MRI findings of the 9 patients with those of 123 patients (25 were pathologically verified) with genetically verified sCJD, which were reported to the Japanese CJD Surveillance Committee.<sup>7</sup> The PRNP analysis revealed that 116 of the 123 had MM129, 5 had MV129, and 2 had valine homozygosity at codon 129. We then compared the features between CJD180 and sCJD by dividing them into two groups: patients with MM129 and patients with MV129.

CSF was examined within 6 months from the onset for the differential diagnosis. The neuron-specific enolase (NSE) value in CSF was measured commercially using an ELISA method (SRL Laboratory, Tokyo, Japan), and a value of >35 ng/mL was considered positive.<sup>8</sup> The 14-3-3 protein immunoassay was performed by western blot using polyclonal antibody SC-629 (Santa Cruz Biotechnology, Santa Cruz, CA). EEG using the International 10–20 method was examined repeatedly during the disease course.

In the MRI study, T1-weighted (T1), T2-weighted (T2), fluid-attenuated inversion recovery (FLAIR), and diffusion-weighted (DWI) imaging was performed for Patients 1, 3, 4, and 5. T1 and T2 were performed for Patients 2, B,<sup>2</sup> and D.<sup>5</sup>

The Mann–Whitney *U* test was used for a comparison of the clinical findings and NSE values between CJD180 and sCJD. The Fisher exact probability test was used for a comparison of the positive rates of clinical symptoms, NSE, 14-3-3 protein, and PSWC.

**Results.** The results of the comparison between CJD180 and sCJD in each group, the MM129 group and MV129 group, are listed in table 2. The two groups had similar results, even though some were not statistically significant. CJD180 had an older onset age, longer duration from the onset to the appearance of myoclonic jerk that was less prominent compared with that of sCJD, longer duration from the onset to becoming akinetic and mute, lower value of NSE in CSF, and lower positive rate of NSE and 14-3-3 protein in CSF compared with those of sCJD. As cardinal symptoms, higher cortical dysfunctions such as aphasia and apraxia, which were not frequent symptoms in sCJD,

From the Department of Neurology (Drs. Jin, Shiga, and Itoyama), Tohoku University School of Medicine, Sendai, Department of Neurology (Dr. Shibuya), Miyagi National Hospital, Yamamoto, Department of Neurology (Dr. Chida), Kohnan Hospital, Sendai, Department of Neurology (Dr. Sato), Research Institute for Brain and Blood Vessels-Akita, Akita, Department of Neurology (Dr. Konno), Nishitaga National Hospital, Sendai, Department of Neuropathology (Dr. Koh-ura), Neurological Institute, Kyushu University Faculty of Medicine, Fukuoka, and Department of Neurological Science (Dr. Kitamoto), Tohoku University School of Medicine, Sendai, Japan.

Presented in part at the 127th annual meeting of the American Neurological Association, New York, NY, October 14, 2002.

Received April 16, 2003. Accepted in final form October 6, 2003.

Address correspondence and reprint requests to Dr. Y. Shiga, Department of Neurology, Tohoku University School of Medicine, 1-1, Seiryomachi, Aoba-ku, Sendai 980-8574, Japan; e-mail: yshiga@em.neurol.med.tohoku.ac.jp

502 Copyright © 2004 by AAN Enterprises, Inc.